Parallel Cortico-Basal Ganglia Mechanisms for Acquisition and Execution of Visuomotor Sequences—A Computational Approach

Hiroyuki Nakahara[1], Kenji Doya[2], and Okihide Hikosaka[3]

Abstract

■ Experimental studies have suggested that many brain areas, including the basal ganglia (BG), contribute to procedural learning. Focusing on the basal ganglia–thalamocortical (BG–TC) system, we propose a computational model to explain how different brain areas work together in procedural learning. The BG–TC system is composed of multiple separate loop circuits. According to our model, two separate BG–TC loops learn a visuomotor sequence concurrently but using different coordinates, one visual, and the other motor. The visual loop includes the dorsolateral prefrontal (DLPF) cortex and the anterior part of the BG, while the motor loop includes the supplementary motor area (SMA) and the posterior BG. The concurrent learning in these loops is based on reinforcement signals carried by dopaminergic (DA) neurons that project divergently to the anterior (''visual'') and posterior (''motor'') parts of the striatum. It is expected, however, that the visual loop learns a sequence faster than the motor loop due to their different coordinates. The difference in learning speed may lead to inconsistent outputs from the visual and motor loops, and this problem is solved by a mechanism called a ''coordinator,'' which adjusts the contribution of the visual and motor loops to a final motor output. The coordinator is assumed to be in the presupplementary motor area (pre-SMA). We hypothesize that the visual and motor loops, with the help of the coordinator, achieve both the quick acquisition of novel sequences and the robust execution of well-learned sequences. A computational model based on the hypothesis is examined in a series of computer simulations, referring to the results of the 2×5 task experiments that have been used on both monkeys and humans. We found that the dual mechanism with the coordinator was superior to the single (visual or motor) mechanism. The model replicated the following essential features of the experimental results: (1) the time course of learning, (2) the effect of opposite hand use, (3) the effect of sequence reversal, and (4) the effects of localized brain inactivations. Our model may account for a common feature of procedural learning: A spatial sequence of discrete actions (subserved by the visual loop) is gradually replaced by a robust motor skill (subserved by the motor loop). ■

INTRODUCTION

Experimental studies on motor learning have shown that many brain areas, including the basal ganglia (BG), are involved in procedural learning (Krakauer, Ghilardi, & Ghez, 1999; Grafton, Hazeltine, & Ivry, 1998; Honda et al., 1998; Karni et al., 1998; Toni, Krams, Turnerd, & Passingham, 1998; Deiber et al., 1997; Brashers-Krug, Shadmehr, & Bizzi, 1996; Curran & Keele, 1993; Passingham, 1993). Some of these areas are preferentially related to the acquisition of novel behaviors, while others are related to the execution of previously learned behaviors (Menon, Glover, & Pfefferbaum, 1998; Petersen, van Mier, Fiez, & Raichle, 1998; Sakai et al., 1998; Jueptner, Frith, Brooks, Frackowiak, & Passingham, 1997; Rauch et al., 1997; Shadmehr & Holcomb, 1997; Doyon, Owen, Petrides, Sziklas, & Evans, 1996; Hikosaka et al., 1996, 2000). These observations have led us to ask the following questions: 1) why are there separate systems for the acquisition of novel behaviors and the execution of learned behaviors?, 2) what computational and representational principles are used in each of them?, and 3) how do they interact with each other? To address these key questions, we have chosen to investigate the cortico-basal ganglia system's role in the acquisition and execution of visuomotor sequences.

The BG are thought to be critically involved in both the learning and control of motor sequences (Graybiel, Aosaki, Flaherty, & Kimura, 1994; Marsden, 1980). They receive inputs from almost the entire cerebral cortex and send projections primarily to the frontal cortex. A striking feature of the BG circuits is that the output of the BG through the thalamus to the cortex is highly topographic, forming separate channels in relation to targeted cortical areas (Hoover & Strick, 1993). At least four basal ganglia–thalamocortical (BG–TC) loops have been identified, namely, the motor, oculomotor, pre-

[1]RIKEN Brain Science Institute, Saitama, Japan, [2]ERATO, JST and ATR International, Japan, [3]Juntendo University, Japan

frontal, and limbic loops (Alexander & Crutcher, 1990). The midbrain dopaminergic (DA) neurons that project heavily to the striatum respond to sensory cues indicating future rewards (Schultz, Apicella, & Ljungberg, 1993; Schultz et al., 1995). This finding led to the proposal that the BG–TC loops work as a reinforcement learning system for learning sequential behaviors and simple reaction tasks by trial and error (Schultz, Dayan, & Montague, 1997; Berns & Sejnowski, 1996; Montague, Dayan, & Sejnowski, 1996; Barto, 1995; Houk, Adams, & Barto, 1995). However, the process by which multiple BG–TC loops work ''together'' is poorly understood. Notably, experiments using the ''2 × 5 task'' (Hikosaka, Rand, Miyachi, & Miyashita, 1995) have shown that the areas within the prefrontal loop are particularly involved in the acquisition of new sequences, whereas the areas within the motor loop are particularly involved in the execution of well-learned sequences (Nakamura, Sakai, & Hikosaka, 1998; Miyachi, Hikosaka, Miyashita, Kardi, & Rand, 1997). Yet, the precise roles of these separate BG–TC loops are still unclear.

The present study investigates how different BG–TC loops work together in visuomotor sequence control by specifically focusing on the representations used within each loop (Hikosaka et al., 1999; Nakahara, 1997; Nakahara, Doya, Hikosaka, & Nagano, 1997). We hypothesize that the (dorsolateral) prefrontal and motor loops learn a visuomotor sequence concurrently but at different speeds, using different representations, based on reinforcement signals provided by the DA neurons; further, the cooperation of the two loops, helped by the pre-supplementary motor area (pre-SMA) that coordinates the contribution of the two loops in a final motor output, achieves both the quick acquisition of novel sequences and the robust execution of well-learned sequences. Simulations using the network model exhibit behavioral characteristics remarkably similar to those in the experimental results of the 2 × 5 task, including the time course of learning (Hikosaka et al., 1995), the effects of sequence reversal and of opposite hand use (Rand, Hikosaka, Miyachi, Lu, & Miyashita, 1998), and the effects of localized inactivation (Nakamura, Sakai, & Hikosaka, 1999; Miyachi et al., 1997).

BACKGROUND

First, we review the experimental findings on the BG–TC loops that are relevant to this study. Second, we summarize the findings on the 2 × 5 task experiments.

Separate Loop Organization of the Basal Ganglia

Among the four major BG–TC loops (Alexander & Crutcher, 1990), the present study focuses on the dorsolateral prefrontal (DLPF) loop and the motor loop. We briefly review the experimental findings of these two loops and, in addition, the pre-SMA. See Table 1.

In the DLPF loop, the projection from the DLPF to the BG terminates mainly in the anterior part of the striatum (caudate head and rostral putamen) (Alexander & Crutcher, 1990; Selemon & Goldman-Rakic, 1985), and

Table 1. Summary of Experimental Results on the Visual and Motor Loops

	Visual Loop	*Motor Loop*
Cortical input[a,b,c,d,e]	DLPF, pre-SMA, IP	SMA, pre-SMA, M1, PM, S1, S2, SP
Striatum[d,f,g]	anterior striatum (dorsolateral head of caudate, rostral putamen)	posterior striatum[a] (posterior putamen)
Cortical target[a,h]	DLPF	SMA, M1, PM
Visual response[i,j,k]	yes	unclear
Eye movement control[j,l,m]	yes	no
Working memory[n,o,p]	yes	no
Motor preparation[i,q,r,s,t]	no	yes
Somatosensory response[r,t,u]	unclear	yes
Laterality of movement control[t]	no	yes (contralateral)
Spinal cord projection[v,w,x]	no	yes

The table emphasizes the contrast between the visual and motor loops but there are exceptions. Abbreviations: DLPF = dorsolateral prefrontal cortex; IP = inferior parietal cortex; pre-SMA = presupplementary motor area; M1 = primary motor cortex; PM = premotor cortex; S1 = primary somatosensory cortex; S2 = somatosensory association cortex; SMA = supplementary motor area; SP = superior parietal cortex.

References: [a]Alexander, DeLong, and Strick (1986); [b]Strick et al. (1995); [c]Bates and Goldman-Rakic (1993); [d]Selemon and Goldman-Rakic (1985); [e]Schmahamann and Pandya (1990); [f]Kemp and Powell (1970); [g]Parent (1990); [h]Hoover and Strick (1993); [i]di Pellegrino and Wise (1993); [j]Andersen et al. (1997); [k]Matsuzaka et al. (1992); [l]Boch and Goldberg (1989); [m]Joseph and Barone (1987); [n]Funahashi et al. (1989); [o]Petrides (1995); [p]Goldman-Rakic (1987); [q]Wise et al. (1997); [r]Rizzolatti et al. (1997); [s]Crammond and Kalaska (1989); [t]Tanji (1994); [u]Mitz and Wise (1987); [v]Hutchins, Martino, and Strick (1988); [w]He, Dum, and Strick (1993); [x]Luppino, Matelli, Camarda, and Rizzolatti (1994).

the projection from the anterior striatum goes back to the DLPF through the thalamus. The posterior parietal cortex, connected with the DLPF, also projects to the anterior striatum. The DLPF is well known to have a visuospatial memory with a working memory characteristic such that information retained by DLPF neurons can be stored temporarily and reset rapidly (Funahashi, Bruce, & Goldman-Rakic, 1989; Goldman-Rakic, 1987). The DLPF plays a role in the control and planning of sequential movements (Watanabe, 1996; Goldman-Rakic, 1987).

The motor loop, which originates from the sensorimotor cortices, such as the primary motor area (M1), the premotor cortex (PM), the supplementary motor area (SMA), and the pre-SMA, runs through the posterior striatum (the middle posterior part of the putamen), and converges mainly in the SMA and also in the PM and M1 (Strick, Dum, & Picard, 1995; Alexander & Crutcher, 1990; Parent, 1990) (see Table 1 for other afferent projections). Compared with the PM and M1, the SMA has been considered to play a role in self-initiated or internally guided movement (Tanji, 1994; Halsband, Ito, Tanji, & Freud, 1993). The SMA primarily receives somatosensory information from the parietal cortex as cortico-cortical inputs and from the BG as major subcortical inputs (Tanji, 1994).

The rostral part of the SMA was recently identified as the pre-SMA (Matsuzaka, Aizawa, & Tanji, 1992). The pre-SMA, not the SMA, is connected with the prefrontal cortex (Tanji, 1994; Matsuzaka et al., 1992). The pre-SMA also receives projections from the rostral cingulate motor area (Bates & Goldman-Rakic, 1993) and modest projections from the inferior parietal lobule (Luppino, Matelli, Camarda, & Rizzolatti, 1993). Thus, the pre-SMA is densely connected with the cortical areas in the DLPF loop (Tanji, 1994; Bates & Goldman-Rakic, 1993), and contains visually responsive neurons (Shima, Mushiake, Saito, & Tanji, 1996; Matsuzaka et al., 1992). At the same time, the pre-SMA is reciprocally connected to the SMA and also shows movement-related activity (Halsband et al., 1993). The pre-SMA sends projections to the bridge regions and its neighboring parts between the anterior and posterior striatum (Takada, Tokuno, Inase, Nambu, & Akazawa, 1997; Parthasarathy, Schall, & Graybiel, 1992).

2 × 5 Task Findings

This section summarizes the procedure and findings of a serial button press task, called the *2 × 5 task experiment* (Hikosaka et al., 1995). We use the simulations of the 2 × 5 task experiment in order to examine our hypothesis on the function of the BG–TC loops. Figure 1A illustrates a sequence of events in a single trial of the 2 × 5 task (see figure legend for details). A single hyperset (a sequence of five sets of two buttons) was used throughout a ''block'' of experiments. A block was considered complete when the number of successful trials reached a criterion (usually 20 or 10). The number of error trials or total trials (i.e., error trials plus a criterion) was used as one of the measures of the performance during a block. Upon completion of a block, a different hyperset was used in the next block. On each training day, the monkey performed about 20 blocks of trials with as many different hypersets. While most hypersets were randomly generated and used only once (called ''new hypersets''), some were used every day (called ''learned hypersets''). The monkeys were able to complete learned hypersets very quickly with very few errors. For each learned hyperset, the monkeys used either their right or left hand throughout the long-term practice.

Short-Term and Long-Term Learning Levels

Sequence learning was found to be composed of at least two learning levels, short-term and long-term: The former was indicated by improved performance ''during a block of experiments'' while the latter was indicated by improved performance ''across days'' (Hikosaka et al., 1995).

Sequences Rather Than Individual Elements are Learned

Rand et al. (1998) used reverse sequences and found that the monkeys acquired learned hypersets as a sequence, not as a collection of separate choices for individual sets (Rand et al., 2000). Such learning was also supported by the finding that eye and hand movements were anticipatory after long-term practice for a particular hyperset (Miyashita, Rand, Miyachi, & Hikosaka, 1996).

Incomplete Transfer of the Learned Skill

Rand et al. (1998) also found that the memory of the learned sequences was only partially accessible to the hand not used for practice; in other words, the skill memory, or a part of the skill memory, is lateralized (Rand et al., 2000).

Functional Differentiation Revealed by Blockade Experiments

To determine the neural correlates of visuomotor sequence learning, an inactivation study (reversible blockade by muscimol injection) was employed. Table 2 summarizes the results for the striatum (Miyachi et al., 1997) and the medial frontal cortex (the pre-SMA and the SMA) (Nakamura et al., 1999) (see legend for details). The results suggest that the anterior BG and the pre-SMA are more involved in the early acquisition of

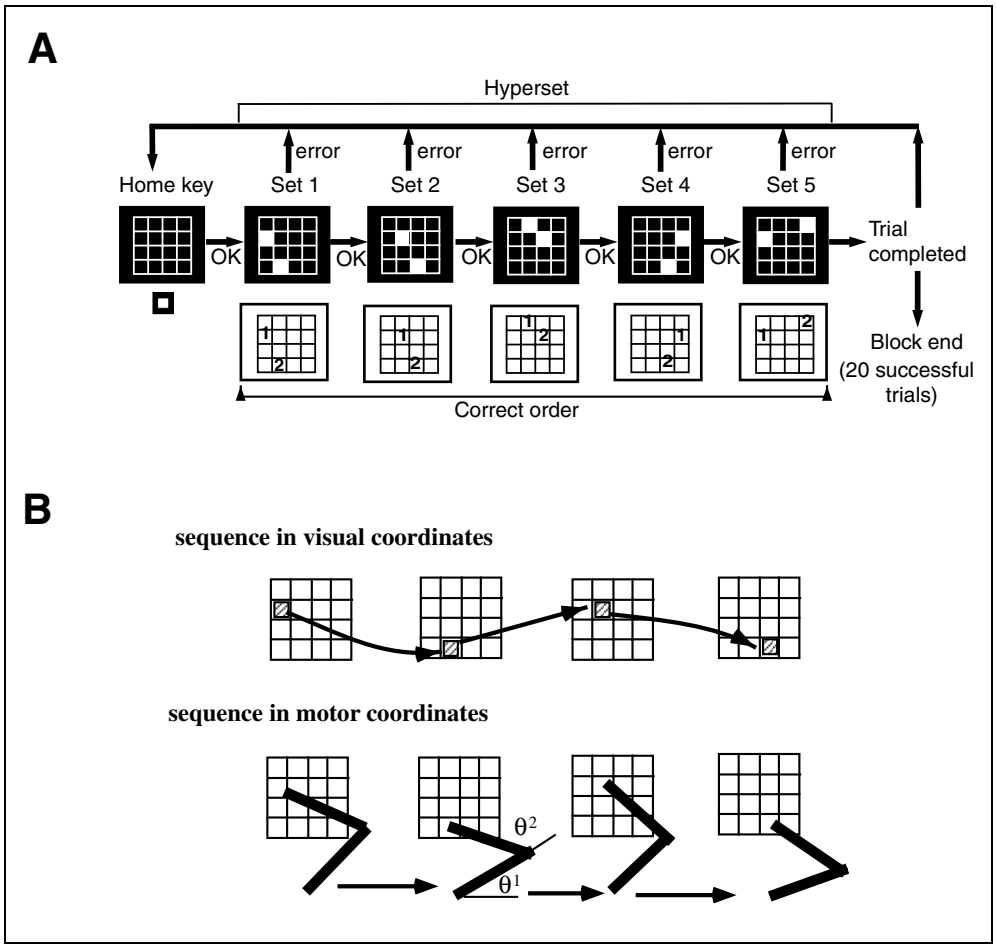

Figure 1. (A) 2 × 5 task with an example of a hyperset. To complete a trial, the monkey has to press 10 buttons (2 buttons × 5 sets) in a predetermined order. When the animal presses the home key at start of trial, 2 out of 16 LED buttons turn on simultaneously, which is a ''set'' of stimuli. The monkey has to determine correct order by trial and error. If successful, another pair of LEDs, the second set, is illuminated and the monkey has to again press buttons in a predetermined order. A fixed sequence of five sets (''hyperset'') is presented in a trial. When the animal presses a wrong button, trial is aborted without a reward, and the animal must start a new trial by pressing the home key. The amount of reward after a successfully completed set gradually increases from the first to final set, so total reward is maximized by completing all sets. (B) An example of two ways of encoding visuomotor sequence in visual or motor representations. The same sequence can be encoded in visual coordinates (top) and in motor coordinates (bottom), e.g., using shoulder and elbow angles in two-dimensional space.

sequence memory, whereas the posterior BG is more involved in the execution/storage.

A MODEL OF THE BASAL GANGLIA LOOPS

In this section, we first briefly explain our hypothesis on the BG loops for visuomotor sequence control, and then introduce a computational model to test the plausibility of the hypothesis. The results of the model's simulations are reported in the next section.

Hypothesis on Visual and Motor Loops

The present study focuses on the two BG loops, namely, the DLPF loop and the motor loop. Our hypothesis on their functions for visuomotor sequence control is based on two propositions (assumptions). The first proposition is that the DLPF and motor loops encode the sequences in visual and motor coordinates, respectively (Table 1 and Figure 2). The visuomotor sequences can be encoded in both representations as a sequence of target positions in visual space (e.g., using head-centered visuospatial coordinates) or of body postures in motor space (e.g., using joint-angle coordinates) (Figure 1B). The DLPF loop also has a working memory capacity (Goldman-Rakic, 1987). Different characteristics between the DLPF and motor loops, reported mainly in physiological experiments using trained animals, support this approximate functional dichotomy (Table 1). From now on, we call the DLPF loop ''the visual loop'' and, for simplicity, consider the SMA as the main cortical area within the motor loop. The second proposition is based on the first one, and holds that visuomotor sequences can be learned faster with the visual loop, while they, once sufficiently learned, can be executed more reliably and more rapidly with the motor loop. This proposition comes from consideration on difference between visual and motor representations in visuomotor sequence tasks (Appendix A) and is implemented in the current model by parameter setting (see below and Motor network in Discussion).

Based on the two propositions above, we hypothesize that the visual and motor loops, as a whole, achieve both the quick acquisition of novel visuomotor sequences and the robust execution of well-learned sequences (Hikosaka et al., 1999; Nakahara, 1997; Nakahara et al., 1997). Both loops can work in a parallel manner, and learn sequences concurrently but at different speeds, using reinforcement signals carried by DA projection. Because of their different speeds, the simple average of

Table 2. Summary of Blockade Experiments Using the 2 × 5 Task

	Learned	*New*
Anterior striatum	↓	↓↓
Posterior striatum[a]	↓↓	–
Pre-SMA	–	↓↓↓
SMA	–	↓

Downward arrow in each cell indicates that performance deteriorated in comparison with normal condition. Data for the anterior and posterior striatum is from Miyachi et al. (1997) and data for the pre-SMA and the SMA from Miyashita et al. (1996). ↓ indicates $p < .05$, ↓↓ $p < .005$, ↓↓↓ $p < .0005$ according to Mann–Whitney U test. Although both blockades of the pre-SMA and the SMA disrupted learning of new hypersets, the pre-SMA blockade induced stronger effects in number of errors, whereas the SMA blockade induced stronger effects in movement parameters. In addition, the bilateral blockade of the SMA slightly but significantly disrupted execution of learned hypersets (Miyashita et al., unpublished observation). We could not directly compare significance of the anterior and posterior striatum with that of the SMA and the pre-SMA, since the former and latter data were taken from different monkeys so control data were also different.

[a]The posterior striatum here refers to the posterior putamen.

the two loops' outputs only compounds the performance of each other. It is then necessary to coordinate the contributions of the two loops in a final motor output. We propose that the pre-SMA acts as a ''coordinator'' between both loops (Figure 2). To take advantage of the strength of each loop, the coordinator should, in principle, guide the whole system to produce a final output by relying primarily on the visual loop in the early stage of learning and on the motor loop in the late stage. Working memory in the DLPF can further accelerate the learning of a new sequence in the visual loop. Working memory has two distinctive characteristics: temporary maintenance and quick resetting of information (Nakahara & Doya, 1998; Baddeley, 1992). The former is helpful for learning a sequence by trial and error. The latter is helpful for switching a task, or learning a sequence one after another, because the quick resetting of information prevents the memories of previously learned sequences from interfering with the learning of a current sequence.

Overall Architecture

To test the plausibility of the above hypothesis, we have constructed a model that captures the basic features of the hypothesis: The model is to (1) have the visual and motor loops work in parallel and concurrently learn sequences using the same reinforcement signal, (2) let the visual loop learn faster than the motor loop, and (3) let the pre-SMA work as a coordinator. This section describes the model without equations; its description with equations is given in subsequent sections.

The network model is based on the anatomical structure of the BG–TC loops and consists of the visual network (visual loop), the motor network (motor loop), the critic network (DA system), and an inverse kinematics module. (The term ''network'' will be used for loop when we refer to our model.) Figure 3A shows the structure of the network model in reference to its anatomical structure (only the cortical parts of the two loops are shown for simplicity; see its legend). Figure 3B shows the structure of the network model in reference to its functional components.

Reinforcement Learning; Actor–Critic Architecture

The model's overall architecture is based on actor–critic architecture that uses a specific type of reinforcement learning algorithm called temporal difference (TD) learning (Barto, 1995). The critic learns to predict cumulative future rewards from a current state (sensory input), whereas the actors learn to produce a motor

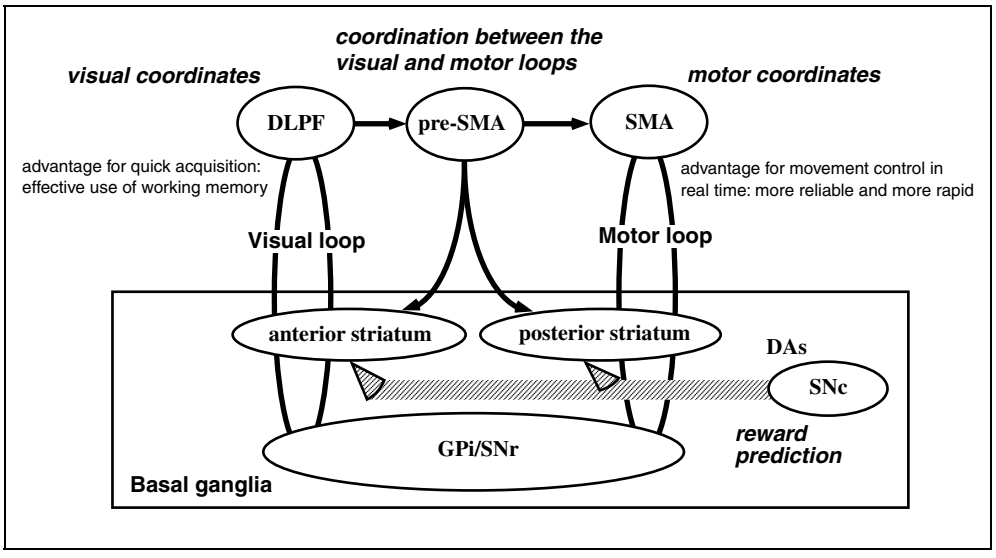

Figure 2. Parallel cortico-basal ganglia mechanisms for acquisition and execution of visuomotor sequences. Visual and motor loops use visual and motor coordinates, respectively. Both visual and motor loops learn visuomotor sequences, using reinforcement signals (i.e., reward prediction errors) provided by DA neurons. Abbreviations: DLPF = dorsolateral prefrontal cortex; pre-SMA = presupplementary motor area; SMA = supplementary motor area; SNc = substantia nigra pars compacta; SNr = substantia nigra pars reticulata; GPi = internal segment of globus pallidus; DAs = dopaminergic neurons.

command that maximizes the cumulative reward. Learning in both the critic and the actors is based on the reward prediction error, called the TD error. As in previous proposals (Schultz et al., 1997; Berns & Sejnowski, 1996; Houk et al., 1995), we assume that the striatum and the substantia nigra pars compacta (SNc) work as the critic network. Specifically, the amount of future reward is predicted by the striatum using the visual input. The DA neurons in the SNc encode the TD error by subtracting the future reward signaled by the striatum from the real reward signaled by the limbic system. In our network model, the visual and motor networks are actors in visual and motor representations, respectively. The parallel architecture in the model allows both networks to concurrently learn sequences.

Functional Components

The visual network contains two functional modules: the visual context prediction and the immediate visual mapping, where the latter has a minimal working memory property (See Figure 3). These two act together to select the spatial position of the LED button (i.e., in visual coordinates). The motor network contains only one module, motor context prediction, and selects the arm posture necessary for pressing the correct button (i.e., in motor coordinates).

The visual (motor) context prediction works in a predictive manner. Thus, it predicts an output in visual (motor) coordinates for a coming input, based upon sequences of previous outputs in visual (motor) coordinates. The immediate visual mapping is reactive and thus produces an output for a current input in visual coordinates. For simplicity, we impose a minimal property of working memory only on the immediate visual mapping (see below).

The pre-SMA is considered to be a coordinator, while the PMv is considered to work as an inverse kinematics module (i.e., the visual-to-motor transformation) (Lu, Preston, & Strick, 1994). Given the pre-SMA response properties (see Discussion), we assumed that the coordinator passes the information on the immediate visual mapping (Figure 3B). At the M1, the final motor output is produced by combining the motor network's output (already in motor coordinates) and the visual network's output, which is transformed as in motor coordinates via an inverse kinematics module.

Details of Visual and Motor Loops

Visual and Motor Representations

Head-centered visual coordinates were used for the visual representation and arm joint-angle coordinates for the motor representation. The state of the visual network was encoded as a 16-dimensional vector in which each component represented the spatial position of the LED button on the panel. The immediate visual input $\boldsymbol{v}^{\mathrm{I}}$ was a binary vector that indicates the illuminated and nonilluminated buttons as 1 and 0, respectively. The state of the motor network was encoded as a 64-dimensional population vector that represented the combination of the shoulder and elbow joint angles (Appendix B). Thus, the motor network learned sequences in motor coordinates that were specific to the effector (i.e., hand).

With two joint-angle motor coordinates, the model was simplified so that an analytic formula could be used in the inverse kinematic module. This module, denoted by $K^{-1}(\cdot)$, transformed the visual vector $\boldsymbol{v}$ into a corresponding populational motor vector $\boldsymbol{m}$ (Appendix B). For a given visual vector $\boldsymbol{v} = (v^1, \ldots, v^{16})$, the corresponding motor vector was given by

$$\boldsymbol{m} = K^{-1}(\boldsymbol{v}) = \sum_{\mathrm{i}=1}^{16} v^i \boldsymbol{m}^i,$$

where $\boldsymbol{m}^i$ was a 64-dimensional vector, corresponding to each v^i in joint angle coordinates.

Prediction of Target Output

The visual and motor networks had the same basic structure:

$$\boldsymbol{v}^{\mathrm{P}}(t) = S(\mathbf{W}^{\mathrm{VI}}\boldsymbol{v}^{\mathrm{I}}(t) + \mathbf{W}^{\mathrm{VC}}\boldsymbol{v}^{\mathrm{C}}(t)),$$

$$\boldsymbol{m}^{\mathrm{P}}(t) = S(\mathbf{W}^{\mathrm{MI}}\boldsymbol{m}^{\mathrm{I}}(t) + \mathbf{W}^{\mathrm{MC}}\boldsymbol{m}^{\mathrm{C}}(t)),$$

where $\boldsymbol{v}^{\mathrm{P}}$ and $\boldsymbol{m}^{\mathrm{P}}$ were the visual and motor target predictions, and $\boldsymbol{v}^{\mathrm{C}}$ and $\boldsymbol{m}^{\mathrm{C}}$ were the visual and motor contexts, respectively. $\boldsymbol{m}^{\mathrm{I}}$ was the vision-based motor input, given by the coordinator (notations for weights and others are given in the legend of Figure 3). S denotes a softmax function:

$$S(\boldsymbol{u})_i \equiv \frac{e^{\zeta u_i}}{\sum_k e^{\zeta u_k}},$$

where ζ is a scaling parameter and $\boldsymbol{u}$ denotes any vector. The softmax function can approximate the action–selection mechanism in the BG, since a sufficiently large value of ζ gives a sharply tuned probability vector (Berns & Sejnowski, 1996; Alexander & Crutcher, 1990).

The visual and motor context vectors, $\boldsymbol{v}^{\mathrm{C}}$ and $\boldsymbol{m}^{\mathrm{C}}$, were constructed from the visual and motor (proprioception) feedbacks of a previous hand position $\boldsymbol{v}^{\mathrm{O}}$ and $\boldsymbol{m}^{\mathrm{O}}$, respectively. These vectors reflected the history of previous actions in visual and motor coordinates, updated as

$$\boldsymbol{v}^{\mathrm{C}}(t+1) = \boldsymbol{v}^{\mathrm{C}}(t) + \frac{1}{\tau_{\mathrm{V}}}(\boldsymbol{v}^{\mathrm{O}}(t) - \boldsymbol{v}^{\mathrm{C}}(t)),$$

$$\boldsymbol{m}^{\mathrm{C}}(t+1) = \boldsymbol{m}^{\mathrm{C}}(t) + \frac{1}{\tau_{\mathrm{M}}}(\boldsymbol{m}^{\mathrm{O}}(t) - \boldsymbol{m}^{\mathrm{C}}(t)),$$

where τ_{V} and τ_{M} were the time constants on the visual and motor contexts.

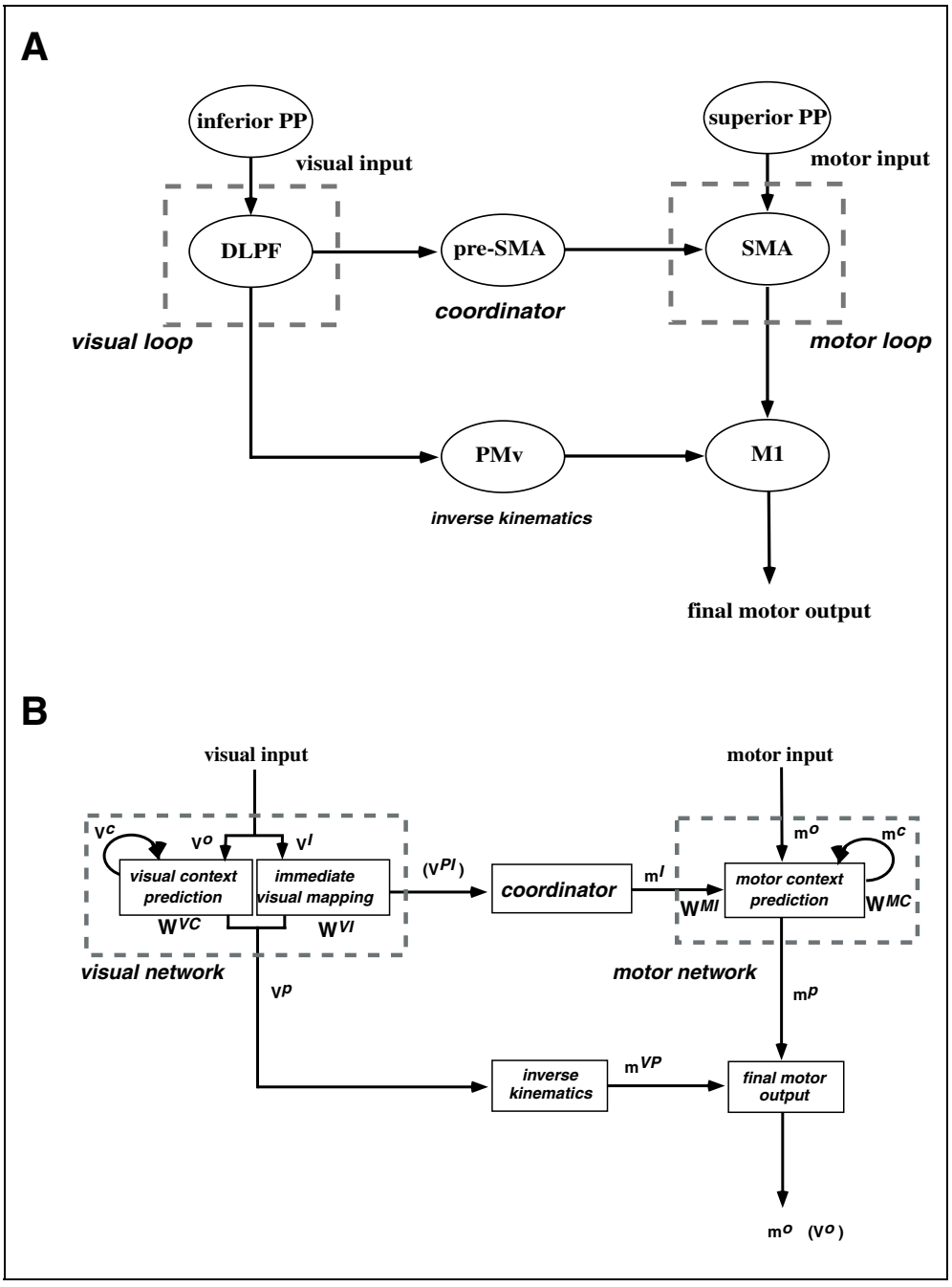

Figure 3. Model network for 2 × 5 task simulation. (A) Anatomical structure and functional modules. The visual network is composed of the DLPF and the anterior BG, whereas the motor network is composed of the SMA and the posterior BG. Visual and motor information is provided to the visual and motor network mainly through the inferior PP (area 7) and through the superior PP (area 5), respectively. Visual and motor contextual information is stored within the DLPF and the SMA, respectively. Two network outputs are generated through the anterior and posterior BG, respectively. The visual network output is assumed to be transformed into a corresponding arm posture through the ventral premotor cortex (PMv) that works as inverse kinematics module, since the DLPF is connected with M1 mainly through the PMv (Lu et al., 1994). Vision-based motor input passes from the visual to the motor network through the pre-SMA that is hypothesized to work as coordinator. The outputs of the PMv and the SMA are combined at the primary motor cortex (M1) to produce final motor command. For the critic network, see subsection on Reinforcement learning algorithm and critic network. Abbreviations: DLPF = dorsolateral prefrontal cortex; pre-SMA = presupplementary motor area; SMA = supplementary motor area; PMv = ventral premotor cortex; M1 = primary motor cortex; PP = posterior parietal cortex; BG = basal ganglia; SNc = substantia nigra pars compacta. (B) Detailed structure of network model. The visual network has two functional modules, the immediate visual mapping and the visual context prediction, while the motor network has one functional module, the motor context prediction. The immediate visual mapping and the visual context prediction are based on immediate visual input $\boldsymbol{v}^{\mathrm{I}}$ and that of visual context $\boldsymbol{v}^{\mathrm{C}}$, respectively. The motor context prediction is based on motor context $\boldsymbol{m}^{\mathrm{C}}$. Abbreviations: $\boldsymbol{v}^{\mathrm{I}}$ = immediate visual input; $\boldsymbol{v}^{\mathrm{C}}$ = visual context; $\boldsymbol{v}^{\mathrm{P}}$ = visual target prediction; $\boldsymbol{v}^{\mathrm{PI}}$ = immediate visual prediction; $\boldsymbol{v}^{\mathrm{O}}$ = visual feedback of hand position; $\boldsymbol{m}^{\mathrm{VP}}$ = vision-based motor target prediction; $\boldsymbol{m}^{\mathrm{I}}$ = vision-based motor input; $\boldsymbol{m}^{\mathrm{C}}$ = motor context; $\boldsymbol{m}^{\mathrm{P}}$ = motor target prediction; $\boldsymbol{m}^{\mathrm{O}}$ = final motor output; $\mathbf{W}^{\mathrm{VI}}$ = weight matrix for immediate visual input; $\mathbf{W}^{\mathrm{VC}}$ = weight matrix for visual context; $\mathbf{W}^{\mathrm{MI}}$ = weight matrix for vision-based motor input; $\mathbf{W}^{\mathrm{VC}}$ = weight matrix for motor context.

Two further constraints were imposed on the network architecture. (1) Working memory function of the DLPF: The function of working memory is to influence decision making by temporarily stored information, or sustained neural activities (Baddeley, 1992; Goldman-Rakic, 1987). Such sustained neural activities can modulate the effective weights of the synaptic inputs by saturating or suppressing some neurons and by activating others. In the present study, the immediate visual mapping is regarded as under the influence of working memory and the result of its learning (i.e., the weight matrix $\mathbf{W}^{\mathrm{VI}}$) was reset at the beginning of each block of a hyperset in imitation of a quick reset of working memory (see Discussion). (2) Coordinator function of the pre-SMA:

The coordinator provides the motor network with the vision-based motor input $\boldsymbol{m}^{\mathrm{I}}(t) = K^{-1}(\boldsymbol{v}^{\mathrm{PI}}(t))$, where $\boldsymbol{v}^{\mathrm{PI}}$ is given by $\boldsymbol{v}^{\mathrm{PI}} = S(\mathbf{W}^{\mathrm{VI}}\boldsymbol{v}^{\mathrm{I}}(t))$. In addition, the weight $\mathbf{W}^{\mathrm{MI}}$ for $\boldsymbol{m}^{\mathrm{I}}(t)$ was kept as an identity matrix for the sake of simplicity, so that $\mathbf{W}^{\mathrm{MI}}\boldsymbol{m}^{\mathrm{I}}(t) = \boldsymbol{m}^{\mathrm{I}}(t)$.

Selection of Final Motor Command

In order to select the final motor command $\boldsymbol{m}^{\mathrm{O}}$, the visual prediction $\boldsymbol{v}^{\mathrm{P}}$ must be transformed into a corresponding arm posture: $\boldsymbol{m}^{\mathrm{VP}} = K^{-1}(\boldsymbol{v}^{\mathrm{P}})$. It was then combined with the motor prediction $\boldsymbol{m}^{\mathrm{P}}$ using a component-wise product:

$$p_j(t) = \frac{m_j^{\mathrm{VP}}(t)m_j^{\mathrm{P}}(t)}{\sum_{k=1}^{64}\mathbf{m}_k^{\mathrm{VP}}(t)\mathbf{m}_k^{\mathrm{P}}(t)} \quad (j = 1, \ldots, 64)$$

One of the 64 motor output units was stochastically selected using the probability distribution $\boldsymbol{p}_j$ and a binary vector $\boldsymbol{m}^{\mathrm{O}}$ was set with only one component as 1. This multiplicative combination, considered as on *e*-geodesic in information geometry (Amari, 1985), gives the sharper output distribution of the two networks than the arithmetic average would (e.g., if the motor network output is uniform, the combined distribution is $p_j = m_j^{\mathrm{VP}}$). Finally, the joint angles encoded by the selected output unit were sent to a two-joint arm model to calculate the hand position. The corresponding visual coordinates were used to set the visual hand position feedback vector $\boldsymbol{v}^{\mathrm{O}}$.

Reward Prediction for Sequence Learning

The critic network performed reward prediction. The goal of the critic learning was to predict the weighted cumulative future reward $P(t) = \sum_{\tau=t}^{T}\gamma^{\tau-t}r(\tau)$, where $r(t)$ was a reward given after action $\boldsymbol{m}^{\mathrm{O}}(t)$ was taken at state $\boldsymbol{v}^{\mathrm{I}}(t)$, T was the end of the trial, and γ was a discount factor, bounded by $0 \leq \gamma \leq 1$. The inconsistency in the prediction was measured by the TD error

$$\hat{r}(t) = r(t) + P(t+1) - P(t) \qquad (1)$$

The cumulative future reward $P(t)$ was predicted by the critic based on the visual input as

$$P(t) = \boldsymbol{w}^{\mathrm{R}} \cdot \boldsymbol{v}^{\mathrm{I}}(t) + b^{\mathrm{R}}$$

The critic weight vector $\boldsymbol{w}^{\mathrm{R}}$ and bias b^{R} were updated to minimize the TD error with

$$\boldsymbol{w}^{\mathrm{R}}(t+1) = \boldsymbol{w}^{\mathrm{R}}(t) + \eta^{\mathrm{R}}\hat{r}(t)\boldsymbol{v}^{\mathrm{I}}(t)$$

$$b^{R}(t+1) = b^{\mathrm{R}}(t) + \eta^{R}\hat{r}(t)$$

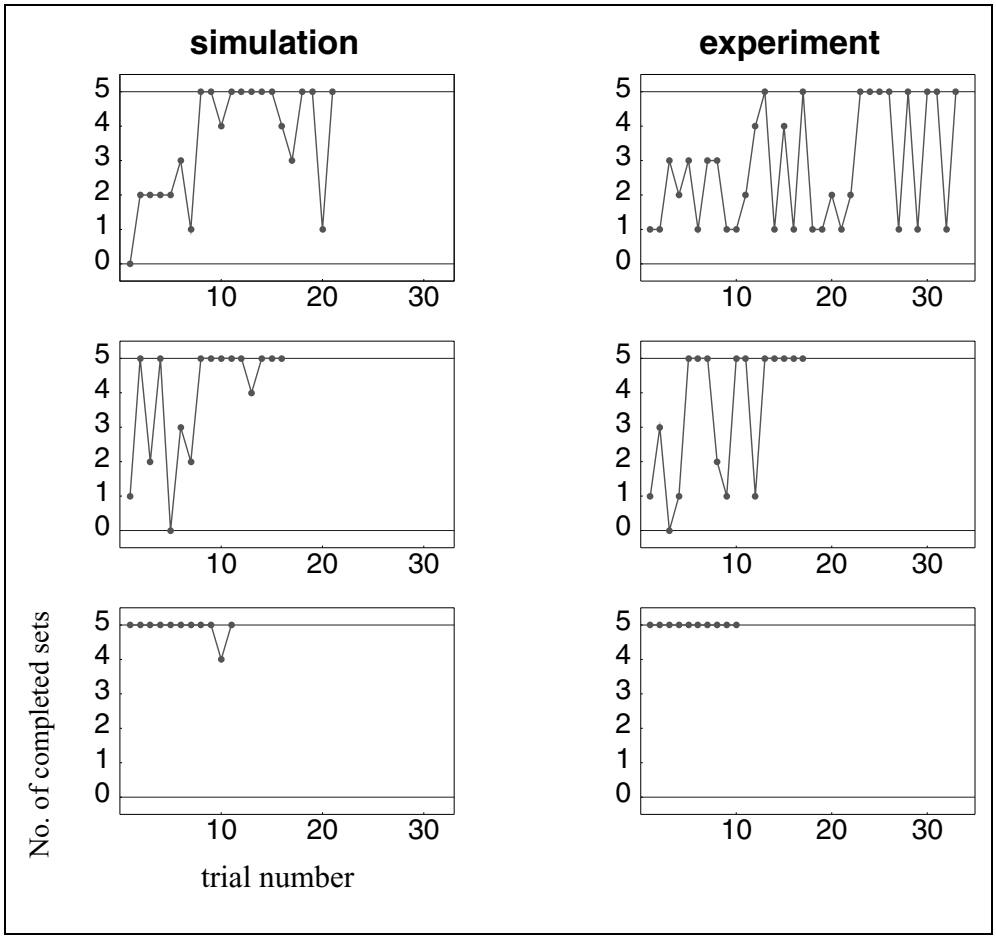

Figure 4. Example of the model's performance in training simulation (left) and monkey's performance in 2 × 5 experiment (right) for a hyperset within a block of trials, compared across three blocks (days). Change in number of completed sets (ordinate) across trials (abscissa) is compared for the first, third, and tenth days from top to bottom. Experimental data is taken from Hikosaka et al. (1995) for a hyperset (no. 176). During each day of the training simulation, we let the model learn three hypersets, two of which were repeatedly used (to be "learned hypersets") and one of which was newly generated every day ("new hypersets"), roughly following the training schedule in the experiment (Hikosaka et al., 1995). A block of trials using one hyperset was completed when the number of successful trials reached the criterion, which we set as 10. Each training simulation was run for 10 days to train the model networks.

In the simulation, the critic network was initialized at the beginning of each block to assure that the resetting of the immediate visual mapping became truly effective. The TD error $\hat{\boldsymbol{r}}(t)$ was also used as a reinforcement signal for the visual and motor networks (Appendix C).

Parameter Setting

We chose specific values for parameters, with some initial values chosen for simplicity, and others chosen by trial and error. In search of other parameters' values, we made sure that the visual network learns faster than the motor network by adjusting the learning speed of each network. We tested how fast either the visual network or the motor network alone learned a new hyperset. Each time the model parameters were reset with their initial states, the test was repeated using different hypersets. The parameters were then chosen to let the visual network learn faster than the motor network (their results are not shown but see the results below). Appendixes C and D provides actual values used in the simulations.

RESULTS OF THE 2 × 5 TASK SIMULATIONS

The simulation results of the model are reported here in reference to the 2 × 5 task experiments. The aim of the simulations is twofold; one is to test if the model indeed reflects the features intended in its construction, such as the role of the coordinator and the importance of the working memory property in the visual loop; the other is to test how the model behaves in simulations in many facets of the 2 × 5 task, in comparison with actual experimental findings on monkeys. Here we report the following results. (1) In training simulations, the model exhibits different levels of learning, short-term and long-term, which are similar to the experimental data (Hikosaka et al., 1995). In addition, the performance of each functional module in the model is presented, indicating that a hypothesized role of each module exists in the model. Furthermore, the importance of the working memory property in the visual loop is also confirmed. (2) A reversed hyperset is as difficult to learn as a new hyperset. (3) The use of the opposite hand results in increased errors with a learned hyperset, but there are still fewer errors than those with a new hyperset. (4) The blockade of model components replicates the results of actual blockade experiments. (5) DA dysfunction in each network indicates the critical role of the visual network in the early stage of learning.

Training Simulation

We first emulated the training period in the simulations, roughly following the experimental schedule (Hikosaka et al., 1995) (see details in Figure 4 legend). At the end of the training period (10 days of the simulation), the model sufficiently acquired the two hypersets (''learned hypersets'') and experienced 10 additional hypersets (''new hypersets''). The results reported below, including other simulations, are averaged over several simulations.

We observed different learning levels, the short-term and long-term learning levels, in the simulation of our model network, which were similar to those observed in experiments (Hikosaka et al., 1995). As shown in Figure 4 (left), the performance of the model for the two hypersets, which were to be learned hypersets, improved ''within'' each block of the simulation experiment, as indicated by the increase in the number of completed sets in later trials (short-term learning). When the model repeatedly practiced the same hyperset, the performance improved ''across'' days so that

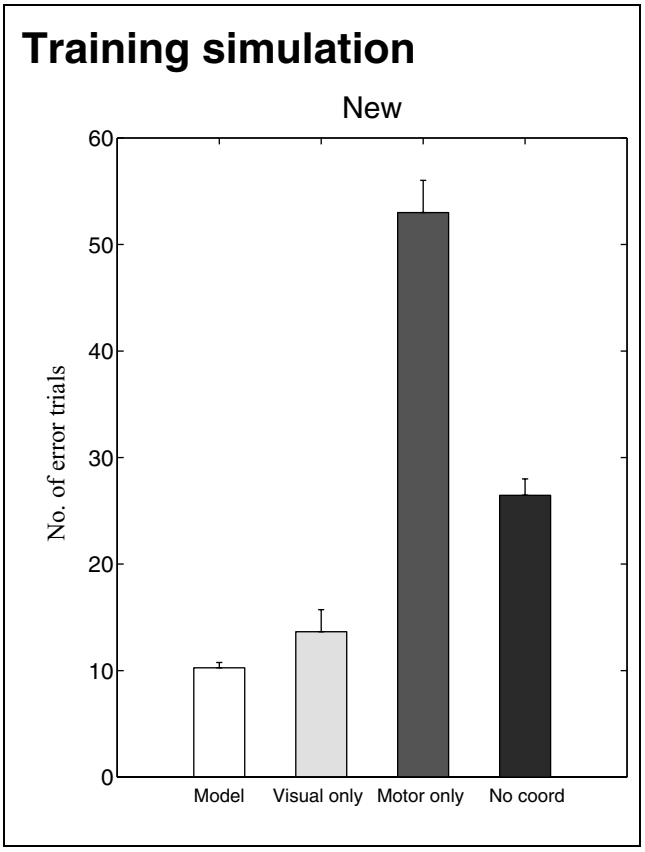

Figure 5. Performance comparisons of proposed model with three architectures, visual-only, motor-only, and no-coordinator for new and learned hypersets in training simulations (represented by Vis-only, Mot-only and No-coord in figure, respectively). The number of errors are shown for new hypersets (error bars stand for *SE*). (1) Visual-only: action probability was only given by visual prediction, i.e., $p_j(t) = m_j^{\mathrm{VP}}(t)$; (2) motor-only: action probability was given by $p_j(t) = m_j^{\mathrm{P}}(t)$ and coordinator used raw visual input instead of visual prediction, i.e., $m^{\mathrm{I}} = K^{-1}(v^{\mathrm{I}})$; (3) no-coordinator: The visual and motor networks are combined without coordinator. All parameters in three architectures are the same as those in the original model. Their performance for new hypersets was measured with new hypersets over 10 simulated days. Performance of learned hypersets in this simulation and that of following simulation with no reset in working memory were measured with learned hypersets on ninth and tenth days, averaged over several training simulations (not shown in the figure).

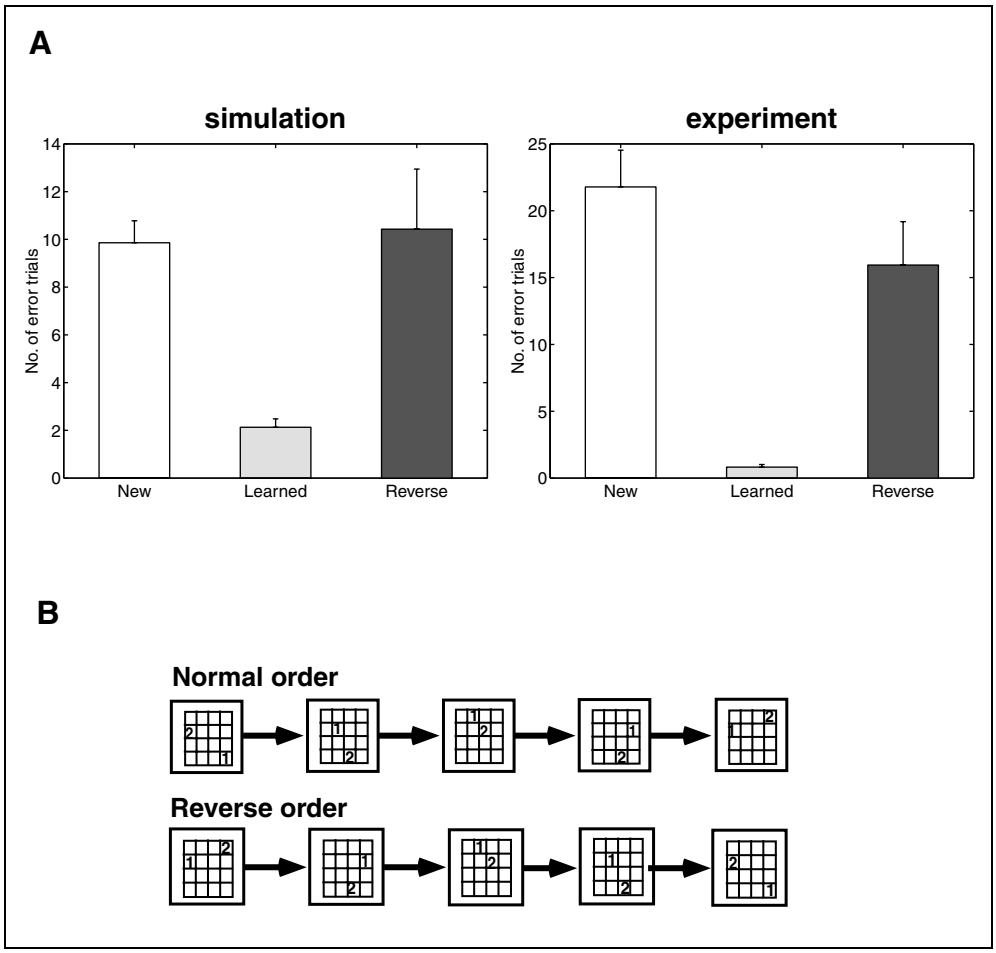

Figure 6. (A) Reversed hyperset simulation (left) and corresponding experimental results (right): Comparison of error trials is shown for new hypersets (white), learned hypersets (gray), and reversed hypersets (black). Experimental data (Monkey KO) taken from Rand et al. (1998). (B) An example of learned hypersets is shown in normal order (above) and reversed order of given learned hyperset above (below).

the hyperset was completed with fewer errors (long-term learning). These results were qualitatively similar to those obtained in the 2 × 5 experiment using monkeys, as shown in Figure 4 (right).

Roles of Individual Functional Modules

It is important to assess how the functional modules in our model, namely, the visual network, the motor network, and the coordinator, contribute to the performance during the training. For this purpose, the training simulations were tested with the following three architectures, the visual-only, the motor-only, and the no-coordinator (Figure 5). We examined their performance for new hypersets over 10 days of simulations. The performance of the model was significantly better than that of the motor-only or that of the no-coordinator (using t test, $p < .0001$ in both cases) and

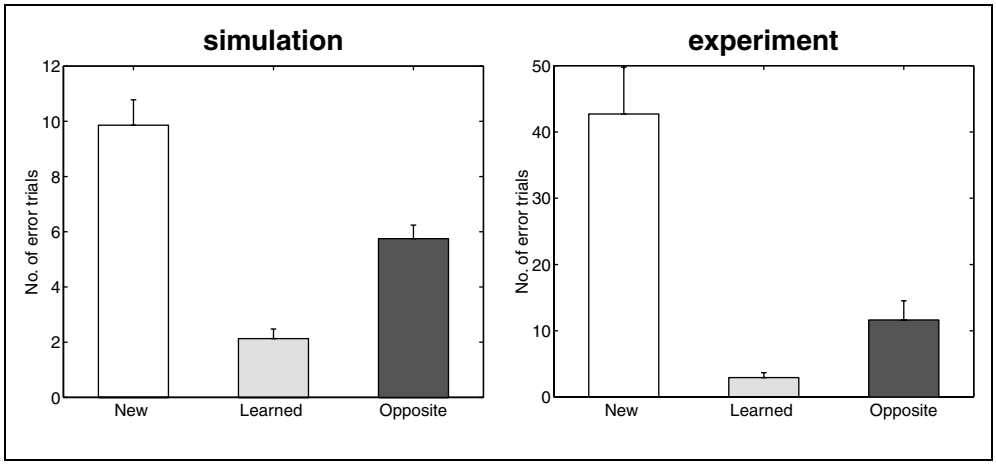

Figure 7. Opposite hand simulation (left) and corresponding experimental results (right): Comparison of error trials by simulating new hypersets (white) and learned hypersets using trained hand (gray) and opposite hand (black). Experimental data (Monkey PI) is taken from Rand et al. (1998).

was comparable (using t test, $p = .058$) but more stable (F ratio test, $p < .00001$) than the performance of the visual-only. The same tendency was observed when we examined the performance for learned hypersets (results are not shown). These results indicate that the model is superior to the three individual architectures. While the visual network learned the new hypersets faster than the motor network, a simple combination of the visual and motor networks (that is, the no-coordinator) led to an intermediate performance. A comparison between the model and the no-coordinator shows that the coordinator significantly improves the performance.

Effect of Working Memory: Reset of Immediate Visual Mapping

As a simplest implementation of working memory, the immediate visual mapping in the visual loop (i.e., $\mathbf{W}^{VI}$) was reset at the beginning of each block. To examine our postulation that a working memory property is helpful in learning new sequences, we tested the simulation in which the immediate visual mapping was not reset in the training simulation. The performances of new and learned hypersets were examined. The simulation results clearly indicate the advantage of resetting the immediate visual mapping. The performance of the model without reset [number of errors: 30.8 (SE ± 4.10)] was worse than the model with reset [number of errors: 10.1 (SE ± .56)] (t test $p < .000001$); no significant effect was found for learned hypersets [with resetting, 2.25 (±.31); without resetting, 3.71 (±.82); $p > .05$]. These results confirmed our postulation.

Reverse Hyperset Simulation

In the training simulation, the model acquired the memories for learned hypersets with long-term practice in manner similar to the monkeys. It was not clear, however, how the memory of learned sequences was stored in the model, specifically whether a hyperset was stored as a sequence or as a collection of individual sets. To differentiate these possibilities, we performed a reverse hyperset simulation, following the experiment (Rand et al., 1998), in which the order of sets in a learned hyperset was reversed while the correct order of button presses remained the same for each set (Figure 6B). The simulation results (Figure 6A, left) show that the performance for reverse hypersets was significantly worse than that for learned hypersets (t test, $p < .0001$), but not significantly different from that for new hypersets. The model network acquired the memory for a learned hyperset as a sequence, replicating the findings of the animal experiment (Figure 6A, right).

Opposite Hand Simulation

An important issue in the study of procedural or motor learning is if the memory is specific to the body part (effector) used for practice or if it can be transferred to

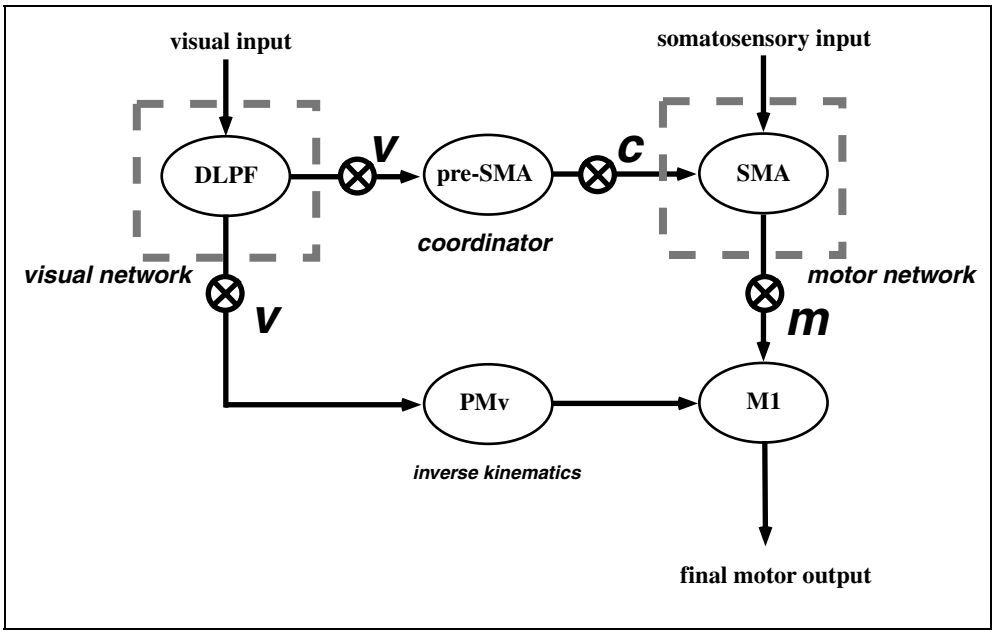

Figure 8. Diagram of blockade simulations: Blocked connection is indicated by ⊗ for each blockade of the visual network (v), the motor network (m), and the coordinator (c). (1) The visual network blockade was realized by suppressing the visual immediate mapping and the visual context prediction. We substituted immediate visual input v^{I} for immediate visual prediction v^{PI} and visual target prediction v^{P}. (2) The motor network blockade was realized by suppressing the motor network; however, visual input was allowed to pass through the motor network. In other words, we let $m^{P}(t) = S(m^{I}(t))$ where $m^{I}(t) = K^{-1}(v^{I}(t))$. (3) The coordinator blockade was realized by allowing only (immediate) visual input to pass to the motor network, that is, we substituted visual input v^{I} for immediate visual prediction v^{PI}. In all three blockades, we let immediate visual input at least pass through even blocked function modules by assuming that those pathways not depicted in our basic model (Figure 3), such as parietal–premotor pathway, may provide information on immediate visual input v^{I} to other function modules.

other body parts. In our model, we postulated that the motor network is present for each effector (each hand) while the visual network is ''bilateral.'' For a simulation of hand transfer, the memory in the visual network was maintained; the memory in the motor network was canceled, but the motor network continued to operate, unlike the blockade simulation below.

The performance for learned hypersets using the opposite hand (Figure 7, left) was significantly worse than that for learned hypersets with the trained hand (t test, $p < .0001$), but significantly better than that for new hypersets ($p < .0005$). These performance results were similar to those obtained in the monkey experiment (Rand et al., 1998; Figure 7, right). The performance for learned hypersets, unlike new hypersets, significantly depended on the motor network. Yet, the memory of learned hypersets stored in the visual network was accessible even when the opposite hand was used so that the performance for learned hypersets was better than that for new hypersets.

Blockade Simulation of Individual Functional Modules

The key feature of our model is that the visual and motor networks acquire the same sequential procedure in parallel but at different speeds, helped by the coordinator. The simulations above confirmed that this feature exists in the model ''during training.'' In order to examine the anatomical correspondence assumed in the model (Figures 2 and 3), we tested the simulation experiments by suppressing the visual network, the motor network, or the coordinator after training simulation. In this way, we emulated the animal experiments in which neural activity was reversibly suppressed by locally injecting muscimol, a GABA agonist (Table 2). These inactivation simulations were also useful in examining how the acquisition and execution of new and learned sequences are allocated in the model after training. Three kinds of inactivation were simulated: blockade of (1) the visual network, (2) of the motor network, and (3) of the coordinator (Figure 8; details of these blockades in the legend).

Figures 9, 10, and 11 show the results from the simulations and from experiments with animals (Nakamura et al., 1999; Miyachi et al., 1997). With the blockade simulation of the visual network (Figure 9), the number of errors significantly increased for new hypersets (t test, $p < .000001$) but showed a less significant increase for learned hypersets ($p < .0001$). In contrast, with the blockade simulation of the motor network (Figure 11), the number of errors significantly

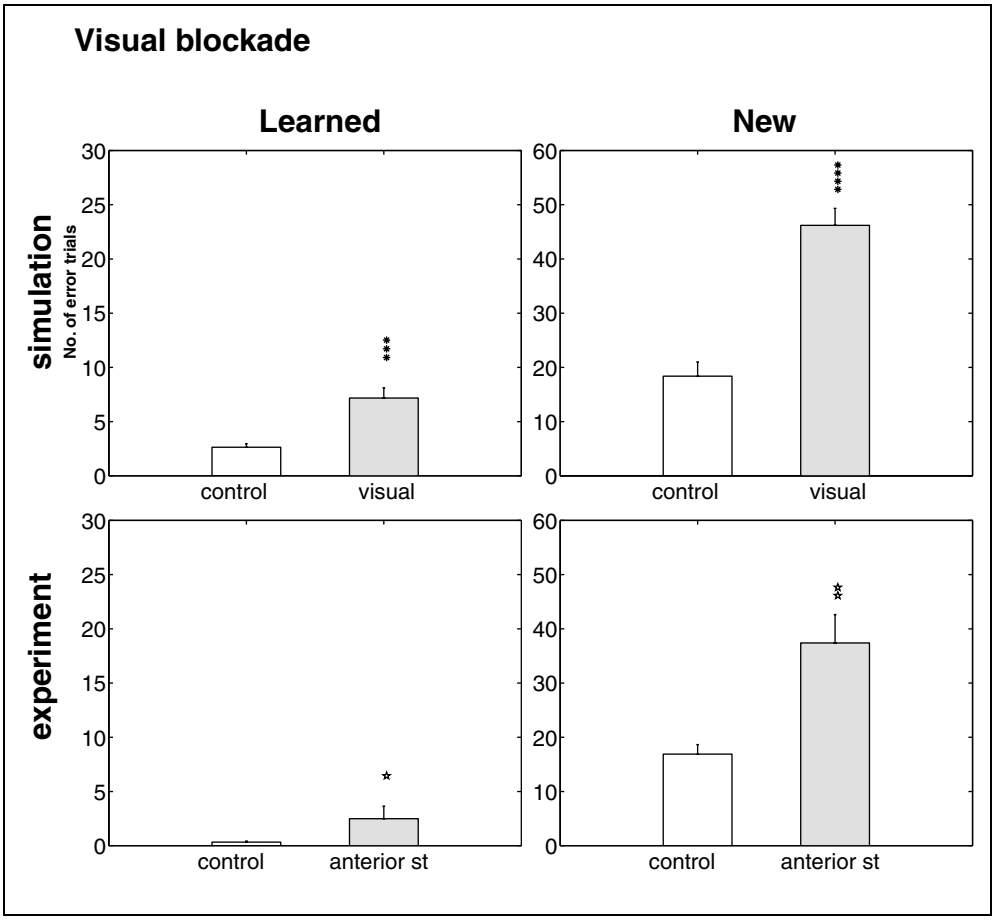

Figure 9. Comparison between simulation of the visual network blockade (top) and experiment (bottom). Error trials are shown for learned hypersets (left) and new hypersets (right). Blockade data (gray) is compared with normal condition (white) in graphs. For experimental data, results of the anterior striatum blockade (Miyachi et al., 1997) are also shown. For this and the following blockade simulation results, according to unpaired t test: * $p < .01$, ** $p < .001$, *** $p < .0001$, **** $p < .00001$ (ns; $p > .05$). For this and the following blockade experimental results, according to Mann–Whitney U test: ⋆ $p < .05$, ⋆⋆ $p < .005$, ⋆⋆⋆ $p < .0005$. The number of trials to the criterion (10 successful trials) under normal conditions in blockade simulation was around 20 for new hypersets. However, in some blockade simulations, the criterion was not achieved even within 100 trials, and the block was then terminated in such cases and treated as if there were 100 trials.

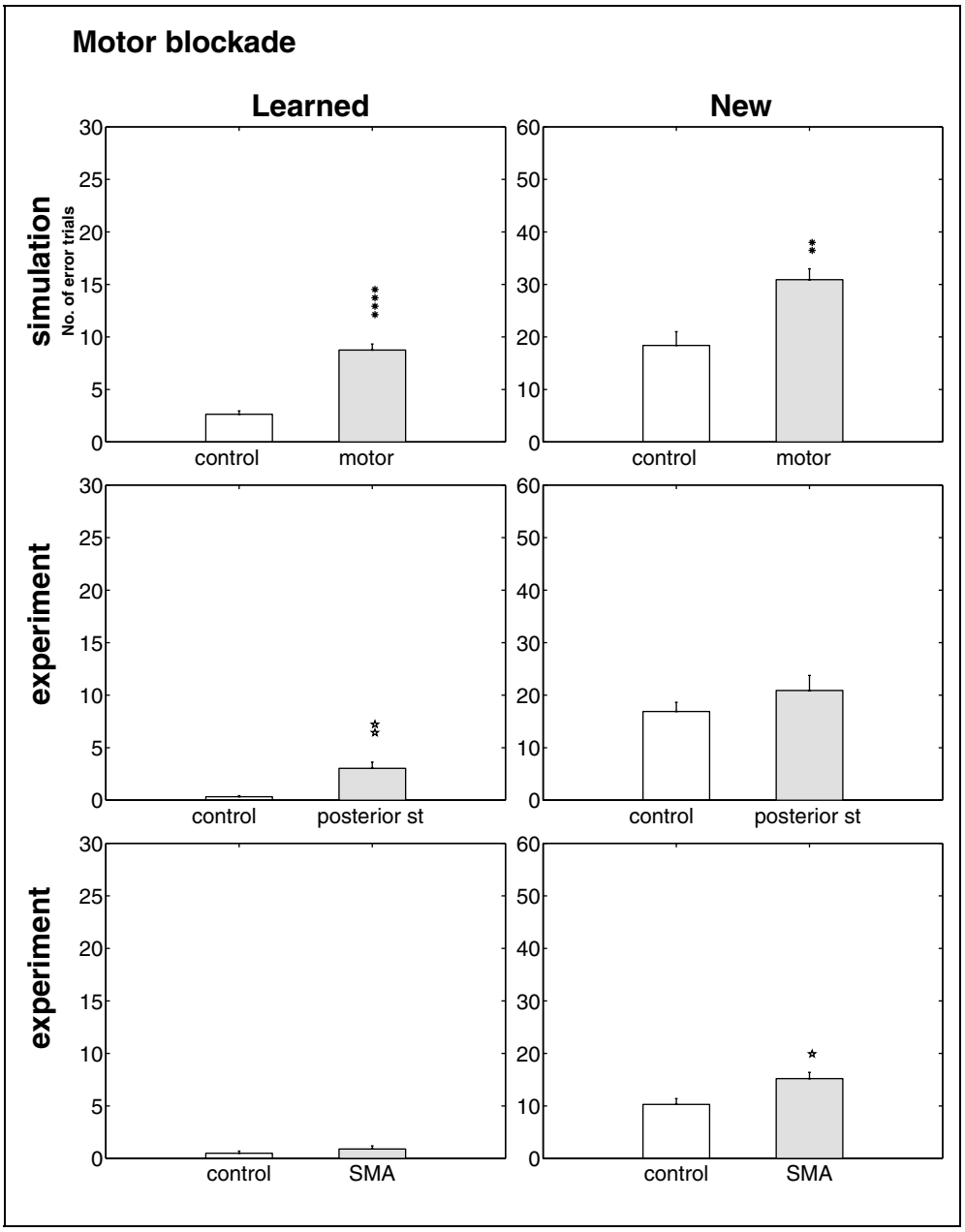

Figure 10. Comparison between simulation of the motor network blockade (top) and experiment (middle, bottom). Error trials are shown for learned hypersets (left) and new hypersets (right). Blockade data (gray) is compared with normal condition (white) on graphs. For experimental data, results of the posterior striatum blockade (Miyachi et al., 1997) and those of the SMA blockade (Miyashita et al., 1996) are also shown (middle and bottom, respectively).

increased for learned hypersets ($p < .000001$) but showed a less significant increase for new hypersets ($p < .001$). The blockade simulation of the coordinator (Figure 11) led to a significant increase in the number of errors only for new hypersets ($p < .001$). These results indicate that the performance of the proposed dual mechanism was superior to the single mechanism (visual or motor network alone). The results further indicate that the visual and motor networks in the model preferentially contributed to the performance for new and learned sequences, respectively, and that the coordinator was selectively related to the performance of new sequences.

We conjectured that the visual network is composed of the loop circuit formed by the DLPF and the anterior part of the BG, while the motor network is composed of the loop circuit formed by the SMA and the posterior part of the BG (Figures 2 and 3). We also assumed that the pre-SMA works as the coordinator. The simulation results are in good agreement with the experimental results (Table 2), given the anatomical correspondence. First, the blockade of the anterior striatum in the monkey experiment (Miyachi et al., 1997), as a part of the visual network, clearly led to deficits in the performance for new hypersets. This was less clear for learned hypersets, and occurred in the same way as the blockade simulation of the visual network (Figure 9). Second, the blockade of the posterior striatum in the monkey experiment (Miyachi et al., 1997), as a part of the

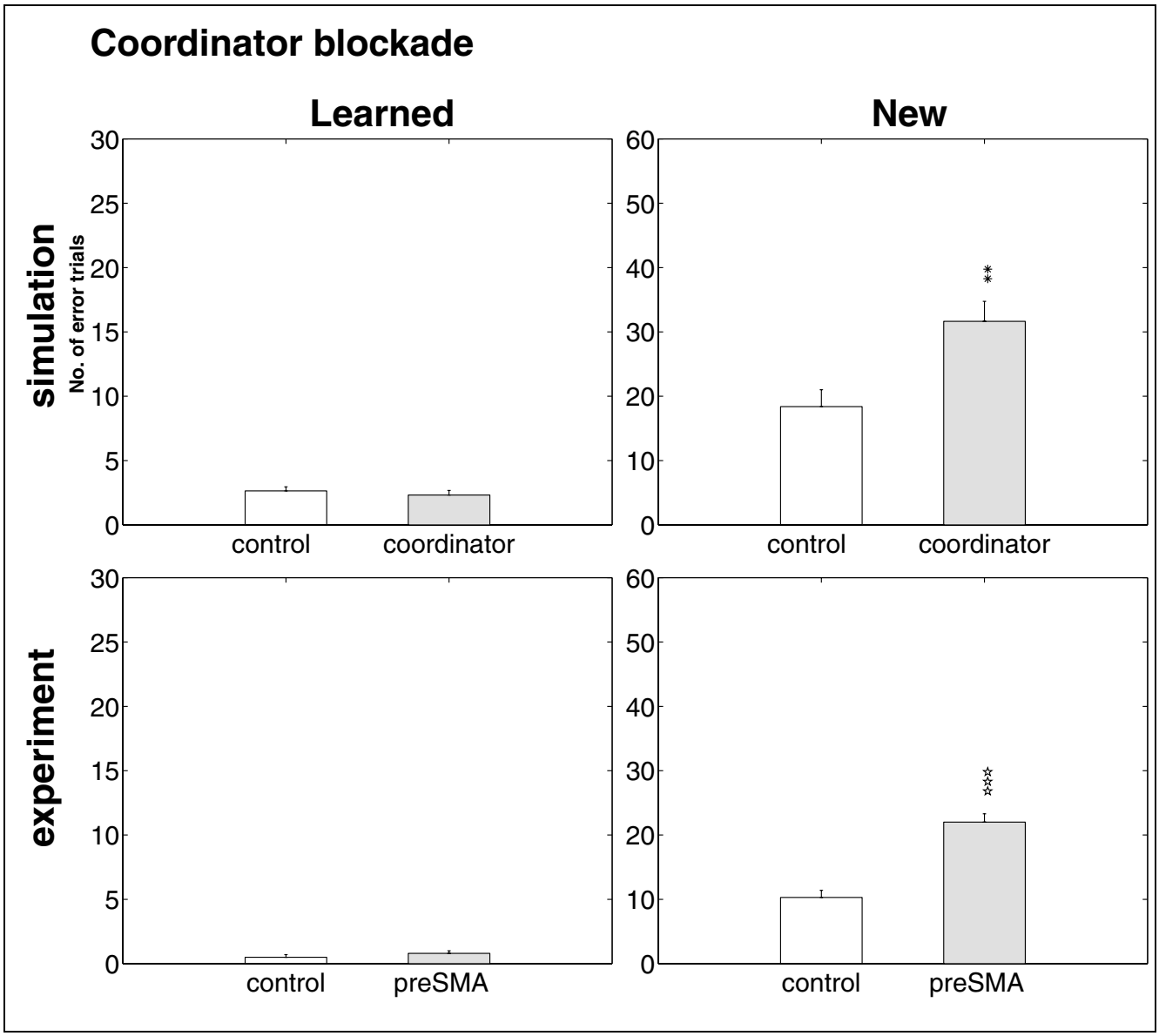

Figure 11. Comparison between simulation of the coordinator blockade (top) and experiment (bottom) Error trials are shown for learned hypersets (left) and new hypersets (right). Blockade data (gray) is compared with normal condition (white). For experimental data, results of the pre-SMA blockade (Miyashita et al., 1996) are also shown.

motor network, led to significant deficits for learned hypersets, but not for new hypersets (Figure 10), while the blockade of the SMA in the monkey experiment (Nakamura et al., 1999), as a part of the motor network, led to deficits for new hypersets but less so than the blockade of the pre-SMA (Figures 10 and 11; also see Table 2 and its legend). The simulation of the motor network blockade roughly corresponds to the results shown in Figure 10: Significant deficits were for both new and learned hypersets, with more severe deficits for learned hypersets than those of the visual network blockade simulation. Third, the blockade of the pre-SMA in the monkey experiment (Nakamura et al., 1999) led to significant deficits for new hypersets but not for learned hypersets, in the same way as the blockade simulation of the coordinator (Figure 11).

DA Dysfunction Simulation: Blockade of Reinforcement Signals

We postulated that the reinforcement signals provided by DA neurons play a critical role in the learning processes of the visual and motor networks. To examine the dysfunction of DA neurons for each network, we simulated the DA dysfunction by simply setting $\hat{r}(t) = 0$ after the model network experienced the training simulations. The DA dysfunction simulations were different from the blockade simulations. In the blockade simulations, the corresponding functional module was basically ''re-

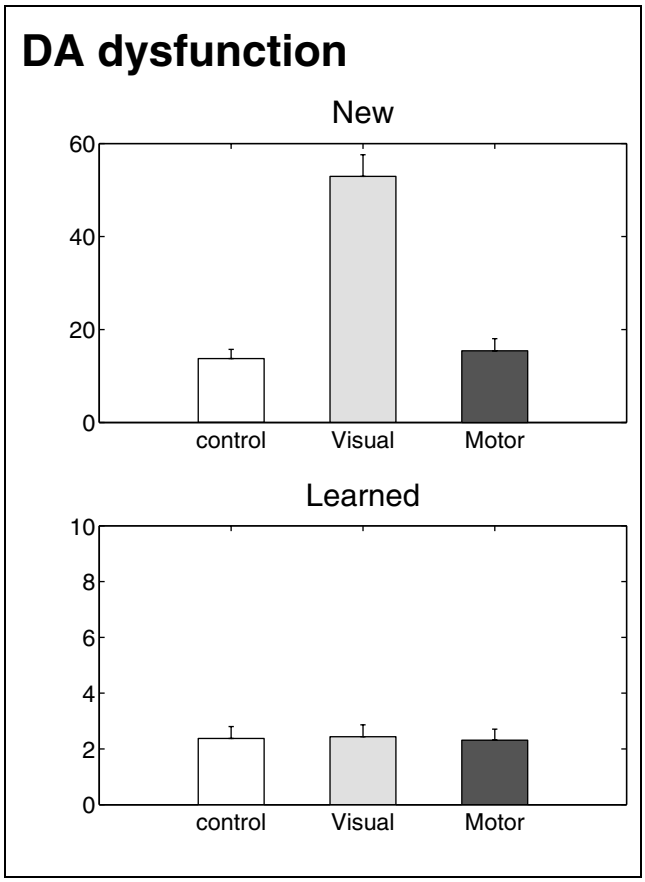

Figure 12. Performance of DA dysfunction simulations: control (left), DA dysfunction in visual network (middle), and DA dysfunction in motor network (right). Error trials are shown for new hypersets (top) and learned hypersets (bottom).

moved,'' so the stored memory in the functional module could not be used in the blockade simulations. On the other hand, in the DA dysfunction simulations, learning in the corresponding functional module was suppressed, yet the already stored memory was still available.

For new hypersets, the performance of the DA dysfunction in the visual network was significantly worse than that of the control ($p < .00001$) (See Figure 12). There was no significant difference between the control and the DA dysfunction in the motor network ($p > .1$). For learned hypersets, there was no significant difference among the three conditions.

DISCUSSION

By focusing on a separate BG–TC loops' architecture (Hoover & Strick, 1993; Alexander & Crutcher, 1990), the present study has investigated how parallel and different time-scale mechanisms, distributed over many brain areas, work together in procedural learning. A computational model is presented and examined with simulations on many facets of the 2 × 5 task experiments (Hikosaka et al., 1995). The assumption, underlying our hypothesis, is that the visual (DLPF) loop, using visual coordinates, acquires a visuomotor sequence faster than the motor loop, using motor coordinates, while the motor loop executes the sequence, once well acquired, more reliably and more rapidly. We have hypothesized that the visual and motor loops can learn a sequence in parallel, using reinforcement signals provided by DA neurons (Schultz et al., 1997; Houk et al., 1995) (Figure 2). The coordinator, assumed in the pre-SMA, adjusts the contribution of the two loops to a final motor output to take advantage of the strength of each loop. With help from the coordinator, the visual and motor loops, as a whole, achieve both the quick acquisition of novel sequences and the robust execution of well-learned sequences (Figure 2).

Our model network based on the hypothesis successfully accounts for the procedural learning process, referred to in 2 × 5 task experiments. The summary of results are as follows. (1) Parallel versus single mechanisms: The performance of the model network is clearly superior to that of either the visual or motor network. The visual and motor networks in the model contribute differentially to the rapid acquisition of new sequences and the long-term storage of well-learned sequences, respectively, shown in inactivation simulations. (2) Coordinator: The coordinator is implemented in the present study as an additional mechanism to pass information from the visual to the motor network. The addition of the coordinator to the visual and motor networks significantly improves the performance in training, indicating that it effectively coordinates the visual and motor networks. (3) Learning processes: The proposed model exhibits different levels of learning in the training period, namely, short-term and long-term learning levels, which have also been found in experiments (Hikosaka et al., 1995). (4) Order selectivity: When the order of stimuli comprising a well-learned sequence is reversed, the model performs no better than with a new sequence, as observed in animal experiments (Rand et al., 1998). The model network acquires a well-learned sequence as a unique sequence rather than a collection of visuomotor mapping. (5) Hand selectivity: When the motor network is reinitialized (reset), the performance of the model network with well-learned sequences deteriorates considerably, yet remained better than that with new sequences. This result matches well with the results of animal experiments on opposite-hand use (Rand et al., 1998, 2000; Miyashita et al., 1996), indicating that the learned sequences strongly depend on a lateralized motor network.

We have also tested the DA dysfunction simulations in each network. The suppression of DA neural signals (reinforcement signals) in the visual network, not in the motor network, affects the acquisition of new sequences, indicating the importance of the visual network for new sequence acquisition. The results also indicate that the performance for well-learned sequences is not deteriorated even when DA dysfunction

occurs in either of the two networks. There is no corresponding experiment in the 2 × 5 task. An experiment may be realized with a local infusion of DA antagonists into the anterior and the posterior striatum for the visual and motor network, respectively.

Characteristics of Parallel Networks for Procedural Learning

The learning of a complex sequential procedure occurs in several steps. Initially, attention mechanisms are required to actively search for correct actions. As the same actions are repeated in a fixed order, the actions are compiled into a unique procedure. After extensive practice, the procedure is performed almost automatically. This attentive-to-automatic process is considered to be a characteristic of procedural learning (Hutchins, 1995; Cohen, Servan-Schreiber, & McLelland, 1992; Anderson, 1982; Fitts, 1964). We suggest that the attentive-to-automatic process of sequential motor control can be understood by considering the parallel network's architecture using different coordinate systems.

Procedural memory can be created concurrently in visual and motor coordinates. Our hypothesis suggests that, in the early stage of learning, the procedure depends primarily on visual coordinates hence, it can be transferred almost perfectly between different effectors. On the other hand, in later stages, performance relies on the memory in motor coordinates, so it is largely effector dependent, although a partial transfer between effectors is possible via the memory in visual coordinates. These predictions on the difference in learning transfer between the early and late stages with respect to different (visual and motor) coordinates transformations have been explicitly tested and confirmed in recent experiments (Rand et al., 2000; Bapi, Doya, & Harner, 1998; see also Rosenbaum, Muelenbroek, & Vaughan, 1999; Willingham, 1998; Imamizu & Shimojo, 1995; Keele & Curran, 1995).

In our model, only the visual network is dependent on working memory and attention so that a subject can attentively learn a new sequence while automatically performing multiple sequences learned with effector-dependent representations. Another implication of the hypothesis is that, in situations where the motor network is better at acquiring sequences (as in a serial reaction-time task), the motor network may guide the visual network in learning the sequences. A subject would start learning without awareness in the early stage of the learning and become aware of the procedure in the late stage (Hikosaka et al., 1999; Honda et al., 1998; Pascual-Leone, Grafman, & Hallet, 1994).

Reinforcement Learning in the BG–TC Loops

The architecture of our model is based on an actor–critic scheme using TD learning, following previous proposals (Suri & Schultz, 1998; Schultz et al., 1997; Berns & Sejnowski, 1996; Barto, 1995; Houk et al., 1995). These proposals are largely based on DA neural responses (Schultz et al., 1993, 1995); however, very few models, based on the proposed scheme, were examined closely with behavioral visuomotor sequence experiments (Berns & Sejnowski, 1996). Our model using TD learning successfully replicates many behavioral results from the 2 × 5 task, while the model's visual and motor networks correspond to ''actors'' in this scheme. This can be considered as a plausibility proof of the scheme.

Recent computational studies, however, have suggested some refinements in the scheme (Daw & Touretzky, 2000; Brown et al., 1999). The current model also ignores the BG's detailed structures, such as direct/indirect pathways (Alexander & Crutcher, 1990) or a striatal compartmental organization (Graybiel et al., 1994), which remain for future studies.

Visual Network

The DLPF and the anterior part of the BG are thought to constitute the main part of the visual loop (Parent, 1990; Selemon & Goldman-Rakic, 1985). When the visual network was inactivated in the simulation, the model's performance deteriorated for both new and learned sequences but especially for new sequences, compared with the motor network inactivation simulations. This result agreed with the experimental results in the inactivation of the anterior striatum (Miyachi et al., 1997; also see Menon et al., 1998). Although the DLPF has not been experimentally inactivated, human imaging studies have shown that the DLPF is activated in the early stage of sequence learning (Honda et al., 1998; Sakai et al., 1998; Jueptner, Stephan, et al., 1997).

In the current model, the working memory property is implemented by resetting only the immediate visual mapping at the beginning of each block, whereas the visual context prediction does not have a working memory property and is treated as long-term memory. The DLPF is known to be involved in maintaining contextual information and sequence planning/learning (Petrides, 1995; Jenkins, Brooks, Nixon, Frackowiak, & Passingham, 1994; Passingham, 1993). This indicates that the working memory property also exists in contextual visual prediction (Monchi & Taylor, 1999; O'Reilly, Braver, & Cohen, 1999; Cohen et al., 1997; Goldman-Rakic, 1987). At the same time, it is more realistic to also consider a long-term visual mapping, or a visual-to-motor mapping that has been suggested to be a function of the dorsal premotor cortex (Wise, Boussaoud, Johnson, & Caminiti, 1997; Kurata & Hoffman, 1994; di Pellegrino & Wise, 1993). Thus, a future model requires elaboration of both the immediate visual mapping and visual context prediction to include both working memory properties and long-term memory.

Eye movement plays a leading role in the performance of learned procedures (Miyashita et al., 1996; Petit et al., 1996; Müri, Rivaud, Vermesch, Léger, & Pierrot-Deseilligny, 1995) and can be considered as mediating visual and motor representations of sequences. Integrating the oculomotor BG–TC loop (Dominey & Arbib, 1992) into the current model is necessary for addressing the issue of hand–eye coordination (Caminiti, Ferraina, & Mayer, 1998). In this regard, we note that the head-centered visuospatial coordinates and the arm joint-angle coordinates were only used as visual and motor representations, respectively, in the current model. The use of other coordinates is necessary not only in visual representation but also in motor representation in a more elaborate model, e.g., eye-, body- and world-centered coordinates as visual representations, and joint-angle trajectories, joint torques, and muscle commands as motor representations (Krakauer et al., 1999; Graziano & Gross, 1998; Andersen, Snyder, Bradley, & Xing, 1997; Rizzolatti, Fogassi, & Gallese, 1997; Wise et al., 1997; Georgopoulos, 1994; Kalaska, Cohen, & Prud'Homme, 1990).

Motor Network

The SMA and the posterior part of the BG are thought to constitute the main part of the motor network in the current model. When the motor network was inactivated in the simulation, the performance of the model deteriorated for both learned and new sequences, but particularly for learned ones, compared with the visual network inactivation simulation. Such deterioration for learned hypersets correlated with the results following an inactivation of the posterior putamen in animal experiments (Miyachi et al., 1997). These results confirm our proposal that the motor network is more critical to the execution of well-learned sequences than the visual network. The SMA results were not completely consistent in the experiment and the simulation. The simulation indicated impairment in both learned and new sequences, while the actual (unilateral) experiment indicated impairment only in new sequences. However, other studies have suggested that the SMA is the storage site of motor memory (Petersen et al., 1998; Jenkins et al., 1994). Alternatively, areas other than the SMA, notably the M1, could prove to be the ultimate storage site for well-learned motor memory (Karni et al., 1998; Nudo, Milliken, Jenkins, & Merzenich, 1996).

We consider that the preferential contribution of the motor network to a well-learned sequence execution comes from this network's slower learning speed under the model's parallel architecture. In training simulations, the model has to perform new sequences one after another and, through repetition of some specific sequences, becomes gradually able to perform very well those sequences (i.e., well-learned sequences). To complete a block of new hypersets, the visual network mainly acquires their sequences, whereas the motor network would need more trials to acquire them. In other words, the memories of the visual network change more rapidly than those of the motor network in completing new hypersets. At the same time, both visual and motor networks gradually acquire the sequences of learned hypersets by repetition. In this process, learning traces of new and learned hypersets are superimposed in each of the two networks. As a net result, we can expect more disturbance of the memory of learned hypersets by acquiring new hypersets in the visual network than in the motor network. Hence, it emerges that the motor network contributes to the robust execution of well-learned sequences.

In the 2 × 5 experiments, measurements included the performance time, the movement time and other parameters, related to real-time motor control (Hikosaka et al., 1995). The performance time for the same hypersets, becoming ''learned hypersets'' after enough experience, decreased across days (Hikosaka et al., 1995). We did not, however, implement the real complexity of the motor coordinates in the current model for simplicity's sake so that we chose two-joint angle coordinates as motor coordinates and used an analytic visual-to-motor transformation. Hence, the current model could not be examined with the parameters, related to real-time motor control. For this investigation, real-time motor control with higher dimensional motor coordinates needs to be implemented. Implementation of higher dimensional motor coordinates will allow us to simulate the effects of nonunique visuomotor transformation on procedural learning. We consider the nonuniqueness in visuomotor transformation (Kawato, 1990; Bernstein, 1967) as a primary reason for the proposition, assumed in the present study, that a visuomotor sequence can be acquired faster in visual coordinates than in motor coordinates (Wolpert, Ghahramani, & Jordan, 1995), while it can be executed, once well acquired, more reliably and more rapidly in motor coordinates (Appendix A) (Rosenbaum et al., 1999; Imamizu, Uno, & Kawato, 1998). Thus, it is important to investigate, with a real-time motor control mechanism in higher dimensional motor coordinates, whether the behavioral parameters of a new model are similar to those measured in the 2 × 5 experiments and whether the above proposition can be justified as we conjectured. Anatomically, a real-time control mechanism presumably includes PMv, M1, and the cerebellum (Sakai et al., 2000; Rizzolatti et al., 1997; Houk & Wise, 1995; Middleton & Strick, 1994; Thach, Mink, Goodkin, & Keating, 1993; Kawato, 1990). In the 2 × 5 experiments, the involvement of the cerebellum, particularly for learned hypersets, has already been shown (Lu, Hikosaka, & Miyachi, 1998).

Coordinator

The pre-SMA is proposed to work as a coordinator. When the coordinator was inactivated in the simula-

tion, the model's performance specifically deteriorated for new sequences in the same way as an inactivation experiment involving the pre-SMA (Nakamura et al., 1999).

Let us discuss how the coordinator in the current implementation realizes its function. The coordinator is implemented as passing information on the immediate visual mapping (a function of a current visual input) to the motor network. Recall that the immediate visual mapping is reset at the beginning of each block. As a result, the information passing through the coordinator to the motor network is the current visual input at the very beginning of each block, and this information gradually becomes the ''correct'' output to the input, as learning of the immediate visual mapping proceeds. The coordinator, thus, inclines the motor network output towards the outputs of the immediate visual mapping. In the motor network, the motor context prediction slowly acquires a sequence over several days of simulations. The motor network output is the sum, passing through the softmax function, of the information from the coordinator and that from the motor context prediction. In other words, this output is determined by the balance of the two forms of information. For a new sequence, the motor context prediction basically produces no output, or a random output because of its memory for previously learned sequences, so that the motor network output is more consistently influenced by the information from the coordinator. For a well-learned sequence, the motor network output is more consistently governed by the motor context prediction. In this manner, the current coordinator influences the motor network output, using the information of the immediate visual mapping (in the visual loop), so that the coordinator can adjust the contributions of the visual and motor loops to the final motor output.

The current implementation of the coordinator is consistent with experimental observations. Anatomically, the pre-SMA can influence the functions of the visual and motor loops (see the Background section). The current coordinator output is closely related to the current visual input; The neural activity in the pre-SMA tends to be more active after receiving sensory inputs and before starting movement, that is, is closely related to the current visual input (Sakai et al., 1999; Halsband, Matsuzaka, & Tani, 1994; Matsuzaka et al., 1992). The number of units is more activated in the current coordinator at the beginning of each block and gradually decays as the visual immediate mapping learns outputs to visual inputs. The pre-SMA is most active when the task is switched (Matsuzaka & Tanji, 1996; Shima et al., 1996) and when sequence learning is in its early stage (Sakai et al., 1998; Hikosaka et al., 1996). The question still remains, however, if such a coordinating function is realized only in pre-SMA or by the interaction of the pre-SMA with some areas, possibly including CMA (Procyk, Tanaka, & Joseph, 2000; Carter et al., 1998; Shima & Tanji, 1998).

Concluding Remark

We have proposed a model consisting of a parallel architecture of the visual and motor loops. The two loops, with the help of the coordinator, acquire and execute visuomotor sequences in procedural learning. The dual mechanism is superior to either mechanism alone and successfully accounts for many aspects of procedural learning that are referred to in 2×5 task experiments, although the model that only focuses on the two BG–TC loops is rather minimal and has many limitations as discussed. Yet, the model extracts an essential feature of procedural learning: A spatial sequence of discrete actions is gradually replaced by a robust motor skill.

APPENDIXES

A. Difference Between Visual and Motor Representations in Visuomotor Sequence Tasks

In the present study, the proposition is assumed that visuomotor sequences can be learned faster with the visual loop, while they, once sufficiently learned, can be executed more reliably and more rapidly with the motor loop. Here, we briefly provide our reasoning for this proposition, based on the difference between visual and motor representations in visuomotor sequence tasks. First, the possible candidates of the targets are given explicitly in visual coordinates in such a task, whereas the candidate target postures are not given explicitly in motor coordinates and are obtained through visual-to-motor transformation. This visuomotor transformation is generally not unique since the dimension to specify target postures in motor coordinates is higher than that to specify targets in visual coordinates. This nonuniqueness makes sequence learning in motor coordinates more difficult than in visual coordinates because the same target position can be represented differently in motor space in different trials (Kawato, 1990; Bernstein, 1967). Second, once a sequence is sufficiently acquired, target postures in the sequence can be optimized, depending on the previous and succeeding target postures, to be executed more reliably and more rapidly, even though this makes learning in motor coordinates further slower than in visual coordinates. On the contrary, if the sequence is executed based on target positions in visual coordinates, the visuomotor transformation is required at every step of movements, which makes execution less accurate and slower. A mathematically rigorous proof is desirable for this reasoning. Studies on on-line learning (Murata & Amari, 1999) suggest that the learning speed has to be set slower in motor coordinates to assure the learning dynamics

stability, given nonunique visuomotor transformation. However, this also remains to be rigorously proved.

B. Visual and Motor Representations

The visual network was encoded as a 16-dimensional vector that encodes 4 × 4 LED positions. The arm was modeled as a planar two joint link with (u^1, u^2) denoting the shoulder and elbow angles. Then, a general relationship between Cartesian hand position (x, y) and the corresponding joint angles (u^1, u^2) was given by

$$x = x_0 + l_1 cos(u^1) + l_2 cos(u^1 + u^2)$$
$$y = y_0 + l_1 sin(u^1) + l_2 sin(u^1 + u^2)$$

where (x_0, y_0) was the position of the shoulder, l_1 was the distance from the shoulder to the elbow, and l_2 was the distance from the elbow to the hand. Thus, for each LED position v^i, whose Cartesian position is (x_i, y_i), the joint angles were given by solving the above equations as

$$u_i^1 = arctan\frac{x_i - x_0}{y_i - y_0} - arccos\frac{l(x_i, y_i)^2 + l_1^2 - l_2^2}{2l_1 l(x_i, y_i)}$$
$$u_i^2 = arctan\frac{x_i - x_0}{y_i - y_0} + arccos\frac{l(x_i, y_i)^2 - l_1^2 + l_2^2}{2l_2 l(x_i, y_i)}$$

where $l(x_i, y_i) =$

The state of the motor network was encoded as a population vector of joint angles in motor coordinates, which we assumed was a vector of normalized Gaussian activation functions for simplicity. A 64-dimensional vector $\boldsymbol{m}^i$, corresponding to (u_i^1, u_i^2), was given by

$$\boldsymbol{m}_j^i = \frac{a_j(\theta_i^1, \theta_i^2)}{\sum_k a_k(\theta_i^1, \theta_i^2)}, (j = 1, \ldots, 64) \quad (2)$$

where

$$a_j(u_i^1, u_i^2) = exp\left\{-\frac{1}{2}\sum_{k=1}^{2}\left(\frac{u_i^k - u_j^k}{\delta^k}\right)^2\right\}$$

$(\hat{u}_j^1, \hat{u}_j^2)$ denotes the preferred shoulder and elbow joint angles for the jth unit and were allocated in the 8 × 8 grid that covered the work area.

C. Reinforcement Learning Algorithm

The inconsistency in the prediction of reward was measured using the TD error (Equation 1). While the TD error $\hat{r}(t)$ was used as a reinforcement signal for the critic, it is also used as a reinforcement signal for the visual and motor networks. The weight matrices $\mathbf{W}^{VI}$, $\mathbf{W}^{VC}$, and $\mathbf{W}^{MC}$ were updated by

$$\mathbf{W}^{VI}(t+1) = \mathbf{W}^{VI}(t) + \eta^{VI}\boldsymbol{r}(t) \cdot G(\boldsymbol{v}^O(t), \boldsymbol{v}^P(t))\boldsymbol{v}^O(t)\boldsymbol{v}^I(t)^T \quad (3)$$

$$\mathbf{W}^{VC}(t+1) = \mathbf{W}^{VC}(t) + \eta^{VC} r(t) \cdot G(\boldsymbol{v}^O(t), \boldsymbol{v}^P(t))\boldsymbol{v}^O(t) \times \boldsymbol{v}^C(t)^T \quad (4)$$

$$\mathbf{W}^{MC}(t+1) = \mathbf{W}^{MC}(t) + \eta^{MC} r(t) \cdot G(\mathbf{m}^O(t), \mathbf{m}^P(t))\mathbf{m}^O(t) \times \mathbf{m}^C(t)^T \quad (5)$$

where η^{VI}, η^{VC}, and η^{MC} were learning rates and were set as 0.2, 0.6, and 0.6 in the simulations, respectively. $G(\mathbf{p},\mathbf{q})$ is the gain matrix for the softmax function. Its ith diagonal matrix components were $(p_i - q_i)q_i(1 - q_i)$ and the rest were zero.

For parameter values of the critic in simulations, we set $\gamma = 0.5$, $\eta^R = 0.2$, $\boldsymbol{w}^R(0) = (-0.4, \ldots, -0.4)$, and $b^R(0) = 1.2$. The reward $\hat{r}(t)$ was zero for the first button of each set and some positive values for the successful second button, increasing from 0.6 for the first set to 1.0 for the fifth set, analogous to the reward schedule in the experiments (Hikosaka et al., 1995).

D. Parameter Values

Here, we summarize the parameter values used in the simulation (also in Appendix C). For the initial values of the weights, we set $\mathbf{W}^{VI}(0)$ as an identity matrix and $\mathbf{W}^{VC}(0)$ and $\mathbf{W}^{MC}(0)$ as zero matrices. The scaling parameter of the softmax function, ζ, was set as 10 and 15 for the visual and motor networks, respectively. For the initial states of the context vectors, we let $\boldsymbol{v}^C(0) = \boldsymbol{v}^I(0)$ and $\boldsymbol{m}^C(0) = \boldsymbol{m}^I(0)$. Time constants τ_V and τ_M for updating $\boldsymbol{v}^C$ and $\boldsymbol{m}^C$ were set as 1.4. Hypersets were generated at random; each of five sets in a hyperset was generated by uniformly choosing 2 buttons of 16 at random. To avoid interference in the first set between learned and new hypersets, we made sure among new hypersets that there is no identical illuminating button pattern with a reverse button-pressing order in the first set, compared with the first set of the learned hypersets.

Acknowledgments

This work was supported by Grant-in-Aid 11780589/12210159 from The Ministry of Education for H.N. and the Uehara Memorial Foundation and JSPS Research for the Future Program for O.H.H.N. acknowledges insights from S. Nagano, S. Miyachi, K. Miyashita, M. K. Rand, S. Sakai, and X. Lu and comments on early drafts from M. Sakagami, S. Amari, J. Lauwereyns, H. Imamizu, R. Bapi, A. Robert, M. W. Miller, and B. Coe.

Reprint requests should be sent to Hiro Nakahara, Laboratory for Mathematical Neuroscience, RIKEN Brain Science Institute, 2-1 Hirosawa, Wako, Saitama, 351-0198, Japan. E-mail: hiro@brain.riken.go.jp.

REFERENCES

Alexander, G. E., & Crutcher, M. D. (1990). Functional architecture of basal ganglia circuits: Neural substrates of parallel processing. *Trends in Neurosciences, 13,* 266–271.

Alexander, G. E., DeLong, M. R., & Strick, P. L. (1986). Parallel organization of functionally segregated circuits linking basal gangla and cortex. *Annual Review of Neuroscience, 9,* 357–381.

Amari, S. (1985). *Differential–geometrical methods in statistics*, vol. 28 of *Springer Lecture Notes in Statistics*. Berlin: Springer.

Andersen, R. A., Snyder, L. H., Bradley, D. C., & Xing, J. (1997). Multimodal representation of space in the posterior parietal cortex and its use in planning movements. *Annual Review of Neuroscience, 20,* 303–330.

Anderson, J. R. (1982). Acquisition of cognitive skill. *Psychological Review, 89,* 369–406.

Baddeley, A. D. (1992). Working memory. *Science, 255,* 556–559.

Bapi, R. S., Doya, K., & Harner, A. (1998). Evidence for effector independent and dependent representations and their differential time course of acquisition during motor sequence learning. *Experimental Brain Research, 132,* 149–162.

Barto, A. G. (1995). Adaptive critics and the basal ganglia. In J. C. Houk, J. L. Davis, & D. G. Beiser (Eds.), *Models of information processing in the basal ganglia* (pp. 215–232). Cambridge: MIT Press.

Bates, J. F., & Goldman-Rakic, P. S. (1993). Prefrontal connections of medial motor areas in the rhesus monkey. *Journal of Comparative Neurology, 336,* 211–228.

Berns, G. S., & Sejnowski, T. J. (1996). How the basal ganglia make decisions. In A. Damasio, H. Damasio, & Y. Christen (Eds.), *Neurobiology of decision-making* (pp. 101–111). Heidelberg, Berlin: Springer-Verlag.

Bernstein, N. (1967). *The coordination and regulation of movements*. London: Pergamon Press.

Boch, R. A., & Goldberg, M. E. (1989). Participation of prefrontal neurons in the preparation of visually guided eye movements in the rhesus monkey. *Journal of Neurophysiology, 61,* 1064–1084.

Brashers-Krug, T., Shadmehr, R., & Bizzi, E. (1996). Consolidation in human motor memory. *Nature, 382,* 252–255.

Brown, J., Bullock, D., & Grossberg, S. (1999). How the basal ganglia use parallel excitatory and inhibitory learning pathways to selectively respond to unexpected rewarding cues. *Journal of Neuroscience, 19,* 10502–10511.

Caminiti, R., Ferraina, S., & Mayer, A. B. (1998). Visuomotor transformations: Early cortical mechanisms of reaching. *Current Opinion in Neurobiology, 8,* 753–761.

Carter, C., Braver, T., Barch, D., Botvinick, M., Noll, D., & Cohen, J. (1998). Anterior cingulate cortex, error detection, and the online monitoring of performance. *Science,* 747–749.

Cohen, J., Perlstein, W., Braver, T., Nystrom, L., Noll, D., Jonides, J., & Smith, E. (1997). Temporal dynamics of brain activation during a working memory task. *Nature, 386,* 604–608.

Cohen, J. D., Servan-Schreiber, D., & McClelland, J. L. (1992). A parallel distributed processing approach to automaticity. *American Journal of Psychology, 105,* 239–269.

Crammond, D. J., & Kalaska, J. F. (1989). Neuronal activity in primate parietal cortex area 5 varies with intended movement direction during an instructed-delay period. *Experimental Brain Research, 76,* 458–462.

Curran, T., & Keele, S. W. (1993). Attentional and nonattentional forms of sequence learning. *Learning, Memory, and Cognition, 19,* 189–202.

Daw, N. D., & Touretzky, D. S. (2000). Behavioral considerations suggest an average reward TD model of the dopamine system. *Neurocomputing, 32–33,* 679–684.

Deiber, M.-P., Wise, S. P., Honda, M., Catalan, M. J., Grafman, J., & Hallett, M. (1997). Frontal and parietal networks for conditional motor learning: A positron emission tomography study. *Journal of Neurophysiology, 78,* 977–991.

di Pellegrino, G., & Wise, S. P. (1993). Visuospatial versus visuomotor activity in the premotor and prefrontal cortex of a primate. *Journal of Neuroscience, 13,* 1227–1243.

Dominey, P. F., & Arbib, M. A. (1992). A cortico–subcortico model for generation of spatially accurate sequential saccades. *Cerebral Cortex, 2,* 153–174.

Doyon, J., Owen, A. M., Petrides, M., Sziklas, V., & Evans, A. (1996). Functional anatomy of visuomotor skill learning in human subjects examined with positron emission tomography. *European Journal of Neuroscience, 8,* 637–648.

Fitts, P. M. (1964). Perceptual-motor skill learning. In A. W. Melton (Ed.), *Categories of human learning* (pp. 243–285). New York: Academic Press.

Funahashi, S., Bruce, C. J., & Goldman-Rakic, P. S. (1989). Mnemonic coding of visual space in the monkey's dorsolateral prefrontal cortex. *Journal of Neurophysiology, 69,* 331–349.

Georgopoulos, A. P. (1994). New concepts in generation of movement. *Neuron, 13,* 257–268.

Goldman-Rakic, P. S. (1987). Circuitry of primate prefrontal cortex and regulation of behavior by representational memory. In F. Plom & V. Mountcastle (Eds.), *Handbook of physiology—The nervous system V*, vol. 5 (chap. 9, pp. 373–417).

Grafton, S. T., Hazeltine, E., & Ivry, R. B. (1998). Abstract and effector-specific representations of motor sequences identified with PET. *Journal of Neuroscience, 18,* 9420–9428.

Graybiel, A. M., Aosaki, T., Flaherty, A., & Kimura, M. (1994). The basal ganglia and adaptive motor control. *Science, 265,* 1826–1831.

Graziano, M. S. A., & Gross, C. G. (1998). Spatial maps for the control of movement. *Current Opinion in Neurobiology, 8,* 195–201.

Halsband, U., Ito, N., Tanji, J., & Freund, H. J. (1993). The role of premotor cortex and the supplementary motor area in the temporal control of movement in man. *Brain, 116,* 243–266.

Halsband, U., Matsuzaka, Y., & Tanji, J. (1994). Neuronal activity in the primate supplementary, pre-supplementary and premotor cortex during externally and internally instructed sequential movements. *Neuroscience Research, 20,* 149–155.

He, S.-Q., Dum, R. P., & Strick, P. L. (1993). Topographic organization of corticospinal projections from the frontal lobe: Motor areas on the lateral surface of the hemisphere. *Journal of Neuroscience, 13,* 952–980.

Hikosaka, O., Nakahara, H., Rand, M., Sakai, K., Lu, X., Nakamura, K., Miyachi, S., & Doya, K. (1999). Parallel neural networks for learning sequential procedures. *Trends in Neuroscience, 22,* 464–471.

Hikosaka, O., Rand, M. K., Miyachi, S., & Miyashita, K. (1995). Learning of sequential movements in the monkey: Process of learning and retention of memory. *Journal of Neurophysiology, 74,* 1652–1661.

Hikosaka, O., Sakai, K., Miyauchi, S., Takino, R., Sasaki, Y., & Pütz, B. (1996). Activation of human pre-SMA in learning of sequential procedures—a functional MRI study. *Journal of Neuropsychology, 76,* 617–621.

Hikosaka, O., Sakai, K., Nakahara, H., Lu, X., Miyachi, S., Nakamura, K., & Rand, M. (2000). *The new cognitive neurosciences* (pp. 553–572). Cambridge: MIT Press.

Honda, M., Deiber, M. P., Ibanez, V., Pascual-Leone, A., Zhuang, P., & Hallett, M. (1998). Dynamic cortical involvement in implicit and explicit motor sequence learning. A PET study. *Brain, 121,* 2159–2173.

Hoover, J. E., & Strick, P. L. (1993). Multiple output channels in the basal ganglia. *Science, 259,* 819–821.

Houk, J. C., Adams, J. L., & Barto, A. G. (1995). A model of how the basal ganglia generate and use neural signals that predict reinforcement. In J. Houk, J. L. Davis, & D. G. Beiser (Eds.),

Models of information processing in the basal ganglia (pp. 249–270). Cambridge: MIT Press.

Houk, J. C., & Wise, S. P. (1995). Distributed modular architectures linking basal ganglia, cerebellum, and cerebral cortex: Their role in planning and controlling action. *Cerebral Cortex, 5,* 95–110.

Hutchins, E. (1995). Cognition in the wild (pp. 287–316). Cambridge: MIT Press.

Hutchins, K. D., Martino, A. M., & Strick, P. L. (1988). Corticospinal projections from the medial wall of the hemisphere. *Experimental Brain Research, 71,* 667–672.

Imamizu, H., & Shimojo, S. (1995). The locus of visual-motor learning at the task or manipulator level: Implications from intermanual transfer. *Journal of Experimental Psychology: Human Perception and Performance, 21,* 719–733.

Imamizu, H., Uno, Y., & Kawato, M. (1998). Adaptive internal model of intrinsic kinematics involved in learning an aiming task. *Journal of Experimental Psychology: Human Perception and Performance, 24,* 812–829.

Jenkins, I. H., Brooks, D. J., Nixon, P. D., Frackowiak, R. S. J., & Passingham, R. E. (1994). Motor sequence learning: A study with positron emission tomography. *Journal of Neuroscience, 14,* 3775–3790.

Joseph, J. P., & Barone, P. (1987). Prefrontal unit activity during a delayed oculomotor task in the monkey. *Experimental Brain Research, 67,* 460–468.

Jueptner, M., Frith, C. D., Brooks, D. J., Frackowiak, R. S. J., & Passingham, R. E. (1997). Anatomy of motor learning: II. Subcortical structures and learning by trial and error. *Journal of Neurophysiology, 77,* 1325–1337.

Jueptner, M., Stephan, K. M., Frith, C. D., Brooks, D. J., Frackowiak, R. S. J., & Passingham, R. E. (1997). Anatomy of motor learning: I. Frontal cortex and attention to action. *Journal of Neurophysiology, 77,* 1313–1324.

Kalaska, J., Cohen, D., & Prud'Homme, M. (1990). Parietal area 5 neuronal activity encodes movement kinematics, not movement dynamics. *Experimental Brain Research, 80,* 351–364.

Karni, A., Meyer, G., Rey-Hipoltio, C., Jezard, P., Adams, M. M., Turner, R., & Ungerleider, L. G. (1998). The acquisition of skilled motor performance: Fast and slow experience-driven changes in primary motor cortex. *Proceedings of the National Academy of Sciences, U.S.A., 95,* 861–868.

Kawato, M. (1990). Computational schemes and neural network models for formation and control of multijoint arm trajectory. In W. T. Miller, R. S. Sutton, & P. J. Werbos (Eds.), *Neural networks for control* (pp. 197–228). Cambridge: MIT Press.

Keele, S. W., & Curran, T. (1995). Modularity of sequence learning systems in humans. *Neural representation of temporal patterns* (pp. 197–225). New York: Plenum.

Kemp, J. M., & Powell, T. P. S. (1970). The corticostriate projection in the monkey. *Brain, 93,* 525–546.

Krakauer, J., Ghilardi, M., & Ghez, C. (1999). Independent learning of internal models for kinematic and dynamic control of reaching. *Nature Neuroscience, 2,* 1026–1031.

Kurata, K., & Hoffman, D. S. (1994). Differential effects of muscimol microinjection into dorsal and ventral aspects of the premotor cortex of monkeys. *Journal of Neurophysiology, 71,* 1151–1164.

Lu, M., Preston, J. B., & Strick, P. L. (1994). Interconnections between the prefrontal cortex and the premotor areas of the frontal lobe. *Journal of Comparative Neurology, 341,* 375–392.

Lu, X., Hikosaka, O., & Miyachi, S. (1998). Role of monkey cerebellar nuclei in skill for sequential movement. *Journal of Neurophysiology, 115,* 2245–2254.

Luppino, G., Matelli, M., Camarda, R., & Rizzolatti, G. (1993). Corticocortical connections of area f3 (SMA-Proper) and are f6 (pre-SMA) in the Macaque monkey. *The Journal of Comparative Neurology, 338,* 114–140.

Luppino, G., Matelli, M., Camarda, R., & Rizzolatti, G. (1994). Corticospinal projections from mesial frontal and cingulate areas in the monkey. *NeuroReport, 5,* 2545–2548.

Marsden, C. (1980, November). The enigma of the basal ganglia and movement. *Trends in Neuroscience,* 284–287.

Matsuzaka, Y., Aizawa, H., & Tanji, J. (1992). A motor area rostral to the supplementary motor area (presupplementary motor area) in the monkey: Neuronal activity during a learned motor task. *Journal of Neurophysiology, 68,* 653–662.

Matsuzaka, Y., & Tanji, J. (1996). Changing directions of forthcoming arm movements: Neuronal activity in the presupplementary and supplementary motor area of monkey cerebral cortex. *Journal of Neurophysiology, 76,* 2327–2342.

Menon, V., Glover, G. H., & Pfefferbaum, A. (1998). Differential activation of dorsal basal ganglia during externally and self paced sequences of arm movements. *NeuroReport, 9,* 1567–1573.

Middleton, F. A., & Strick, P. L. (1994). Anatomical evidence for cerebellar and basal ganglia involvement in higher cognitive functions. *Science, 266,* 458–461.

Mitz, A. R., & Wise, S. P. (1987). The somatotopic organization of the supplementary motor area: Intracortical microstimulation mapping. *Journal of Neuroscience, 7,* 1010–1021.

Miyachi, S., Hikosaka, O., Miyashita, K., Kardi, Z., & Rand, M. K. (1997). Differential roles of monkey striatum in learning of sequential hand movement. *Experimental Brain Research, 115,* 1–5.

Miyashita, K., Rand, M. K., Miyachi, S., & Hikosaka, O. (1996). Anticipatory saccades in sequential procedural learning in monkeys. *Journal of Neurophysiology, 76,* 1361–1366.

Monchi, O., & Taylor, J. G. (1999). A hard wired model of coupled frontal working memories for various tasks. *Information Sciences, 113,* 221–243.

Montague, R., Dayan, P., & Sejnowski, T. J. (1996). Framework for mesencephalic dopamine systems based on predictive hebbian learning. *Journal of Neuroscience, 16,* 1936–1947.

Murata, N., & Amari, S. (1999). Statistical analysis of learning dynamics. *Signal Processing, 74,* 3–28.

Müri, R. M., Rivaud, S., Vermersch, A. I., Léger, J. M., & Pierrot-Deseilligny, C. (1995). Effects of transcranial magnetic stimulation over the region of the supplementary motor area during sequences of memory-guided saccades. *Experimental Brain Research, 104,* 163–166.

Nakahara, H. (1997). *Sequential decision making in biological systems*. PhD thesis, University of Tokyo.

Nakahara, H., & Doya, K. (1998). Near-saddle-node bifurcation behavior as dynamics in working memory for goal-directed behavior. *Neural Computation, 10,* 113–132.

Nakahara, H., Doya, K., Hikosaka, O., & Nagano, S. (1997). Multiple representations in the basal ganglia loops for acquisition and execution of sequential motor control. *Society for Neuroscience Abstracts, 23,* 778.

Nakamura, K., Sakai, K., & Hikosaka, O. (1998). Neuronal activity in medial frontal cortex during learning of sequential procedures. *Journal of Neurophysiology,* 2671–2687.

Nakamura, K., Sakai, K., & Hikosaka, O. (1999). Effects of local inactivation of monkey medial frontal cortex in learning of sequential procedures. *Journal of Neurophysiology,* 1063–1068.

Nudo, R. J., Milliken, G. W., Jenkins, W. M., & Merzenich, M. M. (1996). Use-dependent alterations of movement representations in primary motor cortex of adult squirrel monkeys. *Journal of Neuroscience, 16,* 785–807.

O'Reilly, R. C., Braver, T., & Cohen, J. (1999). A biologically based computational model of working memory. In A. Miyake & P. Shah (Eds.), *Models of working memory* (pp. 375–411). Cambridge: Cambridge University Press.

Parent, A. (1990). Extrinsic connections of the basal ganglia. *Trends in Neurosciences, 13,* 254–258.

Parthasarathy, H. B., Schall, J. D., & Graybiel, A. M. (1992). Distributed but convergent ordering of corticostriatal projections: Analysis of the frontal eye field and the supplementary eye field in the Macaque monkey. *The Journal of Neuroscience, 12,* 4468–4488.

Pascual-Leone, A., Grafman, J., & Hallett, M. (1994). Modulation of cortical motor output maps during development of implicit and explicit knowledge. *Science, 263,* 1287–1289.

Passingham, R. E. (1993). *The frontal lobes and voluntary action,* vol. 21 of *Oxford psychology series*. New York: Oxford University Press.

Petersen, E. S., van Mier, H., Fiez, A. J., & Raichle, E. M. (1998). The effect of practice on the functional anatomy of task performance. *Proceedings of the National Academy of Sciences, U.S.A., 95,* 853–860.

Petit, L., Orssaud, C., Tzourio, N., Crivello, F., Berthoz, A., & Mazoyer, B. (1996). Functional anatomy of a prelearned sequence of horizontal saccades in humans. *Journal of Neuroscience, 16,* 3714–3726.

Petrides, M. (1995). Impairments on nonspatial self-ordered and externally ordered working memory tasks after lesions of the mid-dorsal part of the lateral frontal cortex in the monkey. *Journal of Neuroscience, 15,* 359–375.

Procyk, E., Tanaka, Y. L., & Joseph, J. P. (2000). Anterior cingulate activity during routine and non-routine sequential behaviors in macaques. *Nature Neuroscience, 3,* 502–508.

Rand, M. K., Hikosaka, O., Miyachi, S., Lu, X., & Miyashita, K. (1998). Characteristics of a long-term procedural skill in the monkey. *Experimental Brain Research, 118,* 293–297.

Rand, M., Hikosaka, O., Miyachi, S., Lu, X., Nakamura, K., Kitaguchi, K., & Shimo, Y. (2000). Characteristics of sequential movements during early learning period in monkeys. *Experimental Brain Research, 131,* 293–304.

Rauch, S. L., Whalen, P. J., Savage, C. R., Curran, T., Kendrick, A., Brown, H. D., Bush, G., Breiter, H. C., & Rosen, B. R. (1997). Striatal recruitment during an implicit sequence learning task as measured by functional magnetic resonance imaging. *Human Brain Mapping, 5,* 124–132.

Rizzolatti, G., Fogassi, L., & Gallese, V. (1997). Parietal cortex: From sight to action. *Current Opinion in Neurobiology, 7,* 562–567.

Rosenbaum, D. A., Meulenbroek, R. J., & Vaughan, J. (1999). Remembered positions: Stored locations or stored postures? *Experimental Brain Research, 124,* 503–512.

Sakai, K., Hikosaka, O., Miyauchi, S., Sasaki, Y., Fujimaki, N., & Pütz, B. (1999). Role of pre-SMA in learning of visuo-motor association and motor sequence. *Journal of Neuroscience, 19,* RC1 (1–6).

Sakai, K., Hikosaka, O., Miyauchi, S., Takino, R., Sasaki, Y., & Pütz, B. (1998). Transition of brain activation from frontal to parietal areas in visuo-motor sequence learning. *Journal of Neuroscience, 18,* 1827–1840.

Sakai, K., Hikosaka, O., Takino, R., Miyauchi, S., Nielsen, M., & Tamada, T. (2000). What and when: Parallel and convergent processing in motor control. *Journal of Neuroscience, 20,* 2691–2700.

Schmahamann, J. D., & Pandya, D. N. (1990). Anatomical investigation of projections from thalamus to posterior parietal cortex in the rhesus monkey: A WGA-HRP and fluorescent tracer study. *Journal of Comparative Neurology, 295,* 299–326.

Schultz, W., Apicella, P., & Ljungberg, T. (1993). Responses of monkey dopamine neurons to reward and conditioned stimuli during successive steps of learning a delayed response task. *Journal of Neuroscience, 13,* 900–913.

Schultz, W., Dayan, P, & Montague, R. (1997). A neural substrate of prediction and reward. *Science, 275,* 1593–1599.

Schultz, W., Romo, R., Ljungberg, T., Mirenowicz, J., Hollerman, J. R., & Dickinson, A. (1995). Reward-related signals carried by dopamine neurons. In J. C. Houk, J. L. Davis, & D. G. Beiser (Eds.), *Models of information processing in the basal ganglia* (pp. 231–248). Cambridge: MIT Press.

Selemon, L. D., & Goldman-Rakic, P. S. (1985). Longitudinal topography and interdigitation of corticostriatal projections in the rhesus monkey. *The Journal of Neuroscience, 5,* 776–794.

Shadmehr, R., & Holcomb, H. H. (1997). Neural correlates of motor memory consolidation. *Science, 277,* 821–825.

Shima, K., Mushiake, H., Saito, N., & Tanji, J. (1996). Role for cells in the presupplementary motor area in updating motor plans. *Proceedings of the National Academy of Sciences, U.S.A., 93,* 8694–8698.

Shima, K., & Tanji, J. (1998). Role for cingulate motor area cells in voluntary movement selection based on reward. *Science,* 1335–1338.

Strick, P. L., Dum, R. P., & Picard, N. (1995). Macro-organization of circuits connecting the basal ganglia with the cortical motor areas. In J. Houk et al. (Eds.), *Models of information processing in the basal ganglia* (pp. 117–130). Cambridge: MIT Press.

Suri, R. E., & Schultz, W. (1998). Learning of sequential movements by neural network model with dopamine-like reinforcement signal. *Experimental Brain Research, 121,* 350–354.

Takada, M., Tokuno, H., Inase, M., Nambu, A., & Akazawa, T. (1997). Corticostriatal input from the presupplementary motor area: Its spatial segregation from supplementary motor area. *Neuroscience Research Supplement, 21,* S197.

Tanji, J. (1994, May). The supplementary motor area in the cerebral cortex. *Neuroscience Research, 19,* 251–268.

Thach, W. T., Mink, J. W., Goodkin, H. P., & Keating, J. G. (1993). Combining versus gating motor programs: Differential roles for cerebellum and basal ganglia. In N. Mano, I. Hamada, & M. R. DeLong (Eds.), *Role of the cerebellum and basal ganglia in voluntary movement* (pp. 235–245). Amsterdam: Elsevier.

Toni, I., Krams, M., Turnerd, R., & Passingham, R. E. (1998). The time course of changes during motor sequence learning: A whole-brain fMRI study. *Neuroimage, 8,* 50–61.

Watanabe, M. (1996). Reward expectancy in primate prefrontal neurons. *Nature, 382,* 629–632.

Willingham, D. (1998). A neuropsychological theory of motor skill learning. *Psychological Review, 105,* 558–584.

Wise, S. P., Boussaoud, D., Johnson, B. P., & Caminiti, R. (1997). Premotor and parietal cortex: Corticocortical connectivity and combinatorial computations. *Annual Review of Neuroscience, 20,* 25–42.

Wolpert, D. M., Ghahramani, Z., & Jordan, M. I. (1995). Are arm trajectories planned in kinematic or dynamic coordinates? An adaptation study. *Experimental Brain Research, 103,* 460–470.